Aquaculture 625 (2026) 744325

Contents lists available at ScienceDirect

Aquaculture

journal homepage: www.elsevier.com/locate/aquaculture

Size-dependent salinity tolerance in juvenile stellate sturgeon (*Acipenser stellatus*): Physiological and histopathological responses

Zabih Ollah Pajand [a,*], Esmaeil Hosseinnia [a], Naghmeh Jafari Pastaki [b,c], Ali Hallajian [a], Ayoub Yousefi [a], Arash Lebria [a], Alireza Ashori [a], Hamed Abdollahpour [b,c]

[a] International Sturgeon Research Institute, Iranian Fisheries Science Research Institute, Agricultural Research Education and Extension Organization (AREEO), Rasht, Guilan, Iran
[b] Centro de Ciências do Mar, Universidade do Algarve, Faro, Portugal
[c] Fisheries Department, Faculty of Natural Resources, University of Guilan, Sowmeh Sara, Guilan, Iran

ARTICLE INFO

Keywords:
Acipenser stellatus
Salinity tolerance
Ion regulation
Plasma osmolality
Histopathology

ABSTRACT

We investigated the physiological, endocrine, and histological responses of juvenile stellate sturgeon (*Acipenser stellatus*) to salinity challenge across four weight classes (0.89 ± 0.21, 2.01 ± 0.32, 4.84 ± 0.39, and 9.07 ± 1.47 g; mean ± S.E.) and four salinity levels (0, 4, 8, and 12 ppt) over acute to chronic exposure (3–624 h). A total of 4800 juveniles were used across four sequential experiments, with 100 ± 5 fish per tank (12 tanks per experiment). A replicated factorial design (three tanks per treatment) enabled robust assessment of ionoregulation, stress response, and tissue integrity. Plasma osmolality increased from approximately 230 to 266 mOsm kg^{-1}during early exposure, followed by progressive convergence toward a narrower physiological range (≈251–284 mOsm kg^{-1}) at 624 h, indicating partial osmotic compensation. This adjustment was driven primarily by sodium, which exhibited the strongest salinity- and size-dependent response, confirming its central role in extracellular osmotic regulation. In contrast, potassium displayed pronounced size-dependent dysregulation, with markedly elevated concentrations in fish <3 g during early exposure, reflecting impaired ionic homeostasis and membrane instability, whereas fish >3 g maintained values within or near the physiological range. Cortisol dynamics revealed a clear ontogenetic shift in stress responsiveness. Smaller juveniles (<3 g) exhibited prolonged elevation of cortisol, indicating sustained allostatic load, whereas larger fish (>3 g) demonstrated more efficient recovery, with the 5–10 g group achieving ~92% recovery by 96 h, compared to only ~45% in the smallest size class. These endocrine patterns were consistent with ionoregulatory performance and further support a size-dependent transition in physiological resilience. Histopathological analysis corroborated systemic findings. Histopathological analysis using a semi-quantitative scoring system (0–4) revealed significant size- and salinity-dependent tissue alterations. Gill tissues showed lamellar fusion, epithelial lifting, hyperplasia, necrosis, and hemorrhage, with more severe lesions in smaller juveniles at intermediate to high salinities. Kidney tissues exhibited glomerular expansion, tubular degeneration and obstruction, congestion, hemorrhage, and hemosiderin deposition, with lesion severity generally decreasing with increasing body size. These histological patterns were consistent with physiological and endocrine responses and reflected greater structural resilience in larger juveniles under salinity stress. Collectively, these integrated responses identify an empirical transition zone at approximately 3 g under the tested conditions, below which juveniles exhibit limited capacity to maintain physiological homeostasis under salinity challenge. Above this threshold, fish display more effective physiological regulation, resulting in better ion balance, lower stress, and improved tissue integrity. Together, these findings provide mechanistic evidence for size-based acclimation protocols, gradual salinity transitions, and optimized release strategies to enhance survival and performance in aquaculture and stock enhancement programs.

* Corresponding author.
E-mail address: zpajand@gmail.com (Z.O. Pajand).

https://doi.org/10.1016/j.aquaculture.2026.744325
Received 24 March 2026; Received in revised form 25 May 2026; Accepted 15 June 2026
Available online 17 June 2026

1. Introduction

The Caspian Sea is the principal habitat for sturgeon in northern Iran, and its salinity gradients and hydrological variability create strong physiological challenges for native fishes (Billard and Lecointre, 2000; Xenarios et al., 2025). Sturgeon species are globally threatened because their life histories (large body size, late sexual maturity, and long lifespan) make populations highly vulnerable to overexploitation and habitat change (Jarić et al., 2018; Jafari et al., 2020; Pastaki et al., 2025). Among Caspian *Acipenseridae*, the stellate sturgeon (*Acipenser stellatus*) is an important conservation and commercial species distributed along the southern Caspian coast and is more abundant in the western than in the eastern sector (Sarpanah et al., 2026). This species has experienced substantial population declines in recent decades due to overexploitation, habitat fragmentation, and environmental change, making physiological understanding essential for management and restoration planning (Florescu et al., 2021; Vahdatiraad et al., 2023).

Stellate sturgeon is an anadromous species that migrates between freshwater rivers and brackish and marine waters during its life cycle (Guo et al., 2018), and, like other acipenserids, displays physiological plasticity that enables tolerance across a wide salinity range (Krayushkina and Semenova, 2006; Guo et al., 2018). However, hatchery-reared juveniles often show low post-release survival, suggesting limited capacity to cope with rapid environmental transition. Hatchery programs release juveniles into rivers draining to Caspian Sea, where they encounter variable conditions. In Guilan Province, one of the principal release sites for stellate sturgeon juveniles is the Sefidrud River. The short distance to the sea exposes juveniles to rapid currents, turbidity, low flows, and pollution, which contribute to high post-release mortality (McLean et al., 2016; Wassink et al., 2022). These conditions can result in rapid freshwater–brackish transitions, placing strong demands on osmoregulatory capacity (Allen and Cech Jr, 2007; Allen et al., 2011).

Salinity fluctuations impose osmotic and ionic stress and require rapid physiological adjustment. In euryhaline fish, including sturgeons, exposure to hyperosmotic water typically activates branchial and kidney ion transport mechanisms, and plasma osmolality is often only transiently perturbed. Sturgeon typically maintain plasma osmolality near 250–270 mOsm kg^{-1} across a wide salinity range (McEnroe and Cech Jr., 1985; Downie et al., 2018; Shartau et al., 2023). Molecular studies in Siberian sturgeon (*Acipenser baerii*) further demonstrate regulation of ion transport genes during salinity challenge, indicating conserved osmoregulatory mechanisms in acipenserids (Allen et al., 2009; Guo et al., 2018).

The gills and kidneys are the primary osmoregulatory organs in fish (Barany et al., 2020; Wang et al., 2022). At the gill surface, specialized chloride-cells (ionocytes) perform active salt transport and undergo structural remodelling during salinity acclimation. In Persian sturgeon (*Acipenser persicus*), increased environmental salinity induces proliferation and enlargement of gill chloride-cells accompanied by elevated Na^+/K^+-ATPase (NKA) activity (Shirangi et al., 2016). Similarly, Krayushkina et al. (2015) reported that juvenile stellate sturgeon transferred from freshwater to ≈12–14‰ underwent extensive morpho-functional remodelling of both gill and kidney ionocytes, with elevated NKA activity in both organs and a transient rise in plasma osmolality that was subsequently corrected. Ultrastructural studies also show kidney tubule changes and NKA immunoreactivity consistent with increased ion transport (Taghizadeh Rahmat Abadi et al., 2011).

Systemic measures commonly used to evaluate osmotic status include plasma electrolytes (Na^+, Cl^-, K^+), plasma osmolality, and stress indicators such as plasma cortisol; these parameters provide an integrated view of whole-animal response to environmental change (Kammerer et al., 2010; Abdollahpour et al., 2025). Cortisol, the principal corticosteroid in fishes, has been shown to regulate ion secretion and uptake mechanisms during salinity acclimation in basal ray-finned fishes such as Atlantic sturgeon (*Acipenser oxyrinchus*), supporting the concept that hormonal control of osmoregulation is a conserved vertebrate trait (McCormick et al., 2020). Light and electron microscopy supply complementary structural information on ionocyte remodelling and epithelial adaptation under osmotic stress, enabling interpretation of whether systemic changes reflect regulated acclimation or physiological distress (Abdollahpour et al., 2026).

Osmoregulatory capacity in sturgeons is species-specific, with tolerance to environmental salinity varying among species (Krayushkina and Semenova, 2006; Yuan et al., 2026). Previous studies indicate that salinity tolerance and ionoregulatory performance are strongly influenced by body size and developmental stage. In white sturgeon (*Acipenser transmontanus*), smaller juveniles exposed to elevated salinities exhibit more rapid increases in plasma osmolality and ion concentrations, as well as higher mortality under extreme conditions, compared to larger individuals (Amiri et al., 2009). The selected size classes (0.5–1, 1–3, 3–5, and 5–10 g) were chosen to represent a biologically meaningful ontogenetic gradient and to bracket the size range in which osmoregulatory capacity is known to improve in juvenile sturgeons. Previous studies on Russian sturgeon (*Acipenser gueldenstaedtii*) and *A. persicus* showed that salinity tolerance, plasma ion regulation, cortisol response, and gill chloride-cell maturation increase with body size, with marked improvement occurring at approximately 2.8–3.6 g and above (Krayushkina et al., 1996; Kazemi et al., 2003; Farabi et al., 2011). The smallest class (0.5–1 g), therefore, represents a highly vulnerable early juvenile stage, whereas the 1–3 g class corresponds to the size range commonly used for release in regional sturgeon restoration programs. The 3–5 g and 5–10 g classes were included to test whether larger juveniles exhibit progressively stronger osmoregulatory competence and greater tolerance to salinity challenge, consistent with prior evidence that physiological maturity increases with growth (Krayushkina et al., 1996; Kazemi et al., 2003). Similarly, in green sturgeon (*Acipenser medirostris*), salinity tolerance increases with age and size, with larger juveniles showing higher survival and improved regulatory capacity, accompanied by developmental modulation of plasma osmolality and Na^+/K^+-ATPase activity in osmoregulatory organs (Allen et al., 2009, 2011). Collectively, these findings demonstrate that size, developmental stage, and prior environmental exposure are key determinants of osmoregulatory capacity and survival probability, particularly during post-release environmental transitions.

Despite these advances, important gaps remain. First, systemic plasma indices alone provide an integrated snapshot of osmotic status but cannot resolve the organ-level mechanisms that determine tolerance and recovery. Second, integrated datasets that combine systemic biomarkers (ions, osmolality, cortisol in plasma) with tissue-level evidence (gill and kidney histology and ionoregulatory enzyme activity) remain scarce for juvenile stellate sturgeon exposed to salinities typical of Sefidrud River release sites. Furthermore, the size-dependent integration of systemic and tissue-level responses has not been comprehensively quantified, leaving uncertainty about how developmental stages affect physiological resilience during early post-release transitions. To address these gaps, this study combines biochemical and morphological endpoints across ecologically relevant juvenile size classes and salinity treatments representing conditions between the Sefidrud release site and the adjacent Caspian Sea, where 0 ppt simulated upstream freshwater, 4 and 8 ppt represented transitional estuarine/mixing-zone conditions near the river mouth during seasonal freshwater inflow, and 12 ppt approximated near-sea Caspian salinity (Jamshidi and Abu Bakar, 2012). We measured plasma osmolality, plasma Na^+, K^+, Ca^{2+}, and plasma cortisol, and conducted histological analyses of gill and kidney to detect morpho-functional ionoregulatory responses. We hypothesise that juvenile stellate sturgeons exhibit size-dependent variation in osmoregulatory and endocrine responses to salinity fluctuations, such that smaller individuals have reduced osmoregulatory capacity and delayed endocrine recovery, leading to stronger activation of compensatory tissue remodelling pathways compared with larger cohorts. This integrated approach aims to identify functional size

thresholds and provide practical guidance for release strategies and aquaculture management.

2. Materials and methods

2.1. Animal ethics

All experimental protocols involving animals were reviewed and approved by the Animal Care and Use Committee of the International Sturgeon Research Institute, Agricultural Research, Education and Extension Organization (AREEO), Rasht, Iran. Animal handling and experimental procedures were conducted in accordance with institutional ethical standards, adhered to the ARRIVE guidelines, and were fully compliant with Directive 2010/63/EU of the European Parliament governing the protection of animals used for scientific research.

2.2. Study site and tank

The experiment was conducted at the Guilan Sturgeon Research Station (Chaboksar, Iran; 36°42′N, 51°18′E) using twenty 2-ton circular fibreglass tanks (1.5 m diameter × 1.2 m depth) each equipped with an independent water supply and aeration system. Tanks were fitted with overflow and drain systems to enable controlled water exchange and sampling without crowding or undue handling. Photoperiod followed natural conditions during the experimental month. The experiment was conducted as four sequential trials, one for each juvenile weight class. In each trial, 12 tanks were used simultaneously (4 salinity treatments × 3 replicates), and the tanks were cleaned and reused between trials.

2.3. Experimental animals and allocation

A total of 4800 hatchery-reared stellate sturgeon fingerlings were obtained from the Shahid Beheshti Stock Restoration and Propagation Centre. Fish health status was certified by the hatchery veterinarian according to national health guidelines, and all the fish were of known broodstock origin. Fingerlings were assigned to treatments using randomized allocation within each trial; randomization was performed at the tank level and balanced across salinity treatments to avoid systematic bias. A computer-generated random sequence was used for tank assignment, and allocation was performed by personnel not involved in subsequent sample scoring.

2.4. Experimental design and weight classes

The study used four target salinity treatments (0, 4, 8, 12 ppt) and four juvenile weight classes. Salinity levels were selected to simulate the environmental gradient experienced by released juveniles moving from the Sefidrud River toward the Caspian Sea. The 0 ppt treatment represented upstream freshwater conditions, 4 and 8 ppt represented ecologically relevant transitional salinities that may occur in the estuarine/mixing zone near the river mouth during seasonal discharge, and 12 ppt approximated typical southern Caspian Sea salinity (≈12–13 ppt) (Jamshidi and Abu Bakar, 2012). Fish were allocated into four weight classes based on measured body mass (mean ± S.E.): 0.89 ± 0.21 g, 2.01 ± 0.32 g, 4.84 ± 0.39 g, and 9.07 ± 1.47 g, corresponding to the predefined nominal size ranges of 0.5–1 g (A), 1–3 g (B), 3–5 g (C), and 5–10 g (D), respectively. Each salinity treatment was replicated three times per trial, resulting in 12 tanks per trial and 48 tank-level experimental units across the four sequential trials. Tanks were cleaned and reset between trials. Each tank was stocked with 100 ± 5 fish, corresponding to a nominal density of approximately 50 fish m^{-2}, based on the measured bottom area of the tanks (Fig. 1). Each weight class was tested in a separate sequential trial. Within each trial, the four salinity treatments were replicated three times, resulting in 12 tanks per trial (4 salinities × 3 replicates). Across the four trials, this yielded 48 tank-level experimental units in total.

2.5. Husbandry and water quality

Salinity was achieved by mixing pre-filtered Caspian Sea water (collected 500 m offshore at 5 m depth) with artesian well water and controlled using a computerised dosing system; salinity was verified daily with a calibrated Atago S/mill-E refractometer (±0.1 ppt). Fish were acclimated to treatment salinities at a rate of 1 ppt day^{-1} to minimize osmotic shock, then maintained at target salinities for the experimental period. Water temperature was maintained at 18.4 ± 0.5 °C using heat exchangers and thermostatic control; dissolved oxygen was maintained at 7.34 ± 0.4 mg L^{-1} (≈92.6 ± 4.8% saturation) with continuous aeration and circulation; and pH averaged 7.3 ± 0.6. A controlled water exchange protocol, equivalent to one full volumetric turnover every 24 h, using a flow-through exchange at 1.5 L min^{-1} per kg biomass. The biomass estimates were updated every 48 h (h) to adjust flow rates accordingly and to maintain water quality. Fish were fed live prey (Gammarus spp., *Hediste diversicolor*, chironomid larvae) three

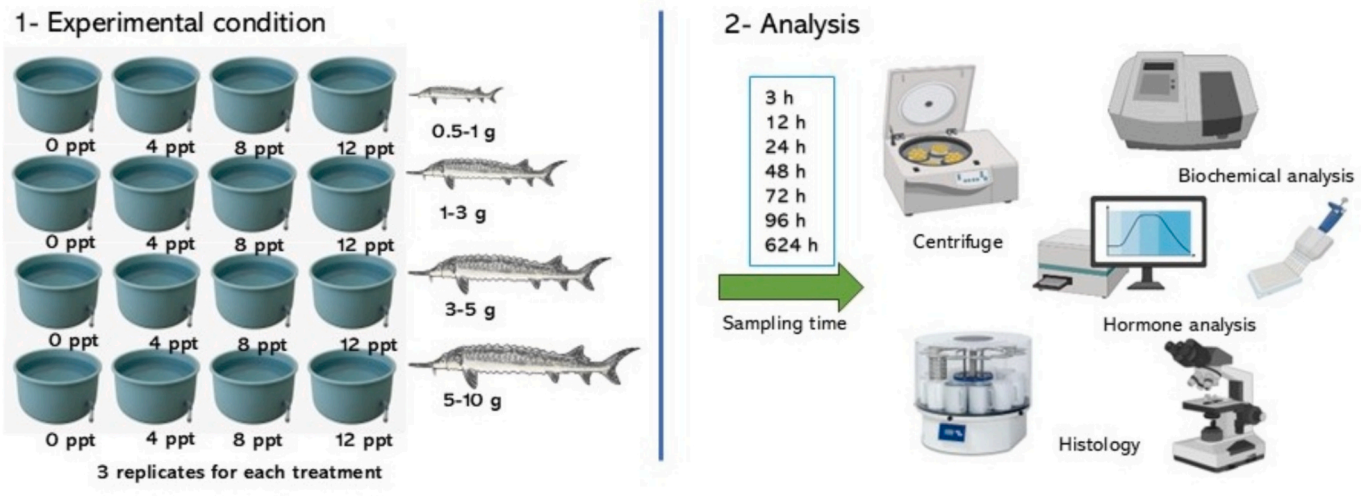

Fig. 1. Experimental design for salinity exposure in juvenile stellate sturgeon (*Acipenser stellatus*). (1) Experimental conditions: Four weight classes (0.5–1 g, 1–3 g, 3–5 g, 5–10 g) were exposed to four salinity levels (0, 4, 8, and 12 ppt) in three replicate tanks per treatment. Each tank was stocked with 50 fish (~50 fish m^{-2}). (2) Analysis: Fish were sampled at multiple time points (3, 12, 24, 48, 72, 96, and 624 h) for biochemical assays, hormone analysis, and histological examination of gill and kidney tissues. Sampling and processing included centrifugation and subsequent laboratory analyses as illustrated.

times daily to apparent satiation (08:00, 13:00, 18:00) (Pajand et al., 2022). The use of live prey followed established sturgeon hatchery protocols in stock enhancement, which recommend natural prey items during early rearing to support feeding behavior.

2.6. Sampling schedule and sample sizes

To minimize postprandial effects on plasma chemistry and cortisol levels, fish were fasted for 24 h before each sampling event. Physiological sampling occurred at seven time points designed to capture acute and chronic responses: 3, 12, 24, 48, 72, 96, and 624 h (≈26 days) after reaching target salinity. However, osmolality was assessed only at 3 and 624 h. At each time point, three fish per tank were randomly netted and sampled; cumulative removals did not exceed 15% of initial stocking density, and remaining densities were within acceptable husbandry limits. The total number of fish sampled for physiological parameters was 336 (4 salinities × 4 weight classes × 7 time points × 3 fish), while osmolality was assessed on 96 fish (4 salinities × 4 weight classes × 2 time points × 3 fish). Mortality was monitored daily and recorded throughout the experimental period.

2.7. Physiological assays and instrumentation

Blood was collected via caudal venipuncture into heparinized microtubes and centrifuged at 3000 ×*g* for 10 min to obtain plasma. Plasma osmolality was measured in triplicate using a calibrated vapour-pressure osmometer (Wescor 5520 or equivalent) with NIST-traceable reference solutions (0 and 300 mOsm kg^{-1}). The interassay coefficient of variation (CV) was <2%. Ion analyses were validated using certified reference materials. Calcium (Ca^{2+}) was quantified by EDTA complexometric titration following ISO 6058. Sodium (Na^{+}) and potassium (K^{+}) concentrations in plasma were determined by flame atomic absorption spectrometry (FAAS; PerkinElmer 3110). Before analysis, plasma samples were appropriately diluted with deionized water to ensure that ion concentrations fell within the linear range of the instrument. Calibration curves for Na^{+} and K^{+} were constructed using certified standard solutions at multiple concentrations (0, 1, 2, 5, and 10 mg L^{-1}), with each curve validated to achieve a correlation coefficient (R^2) > 0.995. Instrumental detection limits were 0.1 mg L^{-1} for Na^{+} and 0.05 mg L^{-1} for K^{+}. All measurements were performed in triplicate. Quality control was maintained by analyzing standard reference solutions after every 10 samples. Chloride (Cl^{-}) was measured using the mercuric thiocyanate method.

Plasma cortisol was quantified using a commercially available ELISA kit (AccuBind ELISA Microwells, Monobind, Inc. Lake Forest, California, USA); the intra-assay and inter-assay coefficients of variation for the cortisol assay were 6.6% and 7.8%, respectively. (Falahatkar et al., 2022). All analyses included blanks and quality controls; technical replicates were used where appropriate. Plasma samples were coded before analysis so that laboratory personnel were blinded to treatment identity during biochemical assays.

2.8. Histology

Histology and semi-quantitative scoring were performed on the gill and kidney. Gill arches and whole kidneys were excised and fixed immediately in 10% neutral-buffered formalin for 24–48 h, dehydrated through graded ethanol, cleared in xylene and embedded in paraffin. Sections were cut at 5 μm thickness, mounted on glass slides and stained with hematoxylin and eosin (H&E) for general morphology; all staining runs included positive tissue controls to ensure staining consistency. Histological examinations and photomicrography were performed using a light microscope (Olympus BX51, Tokyo, Japan), and representative images were captured at 20× and 40× magnification. Semi-quantitative scoring used a uniform 0–4 rubric for both organs (0 = none; 1 = mild; 2 = moderate; 3 = marked; 4 = severe). Lesion categories were predefined for the gill (adhesion, hyperplasia, necrosis, congestion, hemorrhage, epithelial detachment, clubbing, hemosiderin) and the kidney (glomerular expansion, tubular necrosis, hypertrophy, congestion, hemorrhage, lymphoid/hematopoietic proliferation, hemosiderin). All slides were coded before scoring, and histological evaluation was performed blinded to salinity and weight class. For each section, 10 random non-overlapping fields were examined.

2.9. Statistical analysis

All statistical analyses were performed using R version 4.4.3 (R Core Team, 2024) within RStudio. The following R packages were utilized: lme4 (v1.1–35) and lmerTest (v3.1–3) for mixed-effects models; emmeans (v1.10.0) for post-hoc comparisons; multcomp (v1.4–25) and multcompView (v0.1–9) for compact letter displays; car (v3.1–2) for Levene's test; performance (v0.10.0) for model diagnostics; MuMIn (v1.47.5) for marginal and conditional R^2 calculations; ggplot2 (v3.4.4) for data visualization; and dplyr (v1.1.4) and tidyr (v1.3.0) for data manipulation. Significance was set at $\alpha = 0.05$ for all tests.

For each physiological variable (plasma osmolality, Na^{+}, K^{+}, Ca^{2+}, Cl^{-}, cortisol) and mortality, linear mixed-effects models were fitted as: Response ~ Salinity × WeightClass × Time + (1 | TankID) to account for the hierarchical design (fish nested within tanks). Mortality data were analyzed using a two-way ANOVA (Salinity × WeightClass) after arcsine-square root transformation to meet normality assumptions. Models were estimated by Restricted Maximum Likelihood (REML), and fixed-effect significance was assessed using Type III ANOVA with Satterthwaite degrees-of-freedom approximation (lmerTest). Model assumptions (normality of residuals, homogeneity of variances) were verified using Shapiro-Wilk tests and Levene's tests, respectively; where assumptions were violated, data were log-transformed or non-parametric alternatives (Kruskal-Wallis) were employed.

Post-hoc pairwise comparisons were computed as estimated marginal means with Tukey adjustment for family-wise error (emmeans); results were reported as compact letter displays (multcompView) where groups sharing the same letter are not significantly different ($p > 0.05$). Where many exploratory contrasts were performed, we applied Benjamini–Hochberg false-discovery rate control. Model fit and assumptions were evaluated using simulation-based residual diagnostics (DHARMa) and checks for homoscedasticity and normality; model performance was summarized with marginal and conditional R^2 (MuMIn) and random-effect variances (including ICC) were reported. Time was treated as a categorical factor to permit detection of non-linear temporal responses across sampling points.

2.9.1. Exploratory composite indices and derived analyses

Allometric relationships between body size and ion regulation were assessed using Pearson correlation coefficients. Physiological stability across salinities was quantified as the coefficient of variation (CV = SD/mean × 100) calculated across the four salinity treatments for each parameter within each weight class. The Osmoregulatory Efficiency Index (OEI) was developed as a composite measure of ionoregulatory health: OEI = 100 – (Na_dev + K_dev + Cl_dev)/3, where deviation = |measured – ideal|/ideal × 100.

The "ideal" values were defined as 100 mmol/L for Na^{+} and Cl^{-}, and 4 mmol/L for K^{+}. These values are consistent with typical plasma ion concentrations reported for healthy freshwater-adapted sturgeons and general teleost physiology (McCormick, 2001; Evans et al., 2005; Krayushkina and Semenova, 2006). Furthermore, they were empirically confirmed as the mean plasma concentrations measured in the largest, fully adapted fish (5–10 g weight class maintained in freshwater, 0 ppt) at the conclusion of the experiment (624 h), representing the most stable and unstressed physiological condition. Both approaches converge on the same set points (Na^{+}: 90–110 mmol/L, Cl^{-}: 90–110 mmol/L, K^{+}: 3–5 mmol/L). While the absolute ideal may vary slightly among individuals or conditions, the OEI provides a standardized, relative

measure of ionoregulatory competence; larger deviations from the ideal indicate poorer regulation regardless of species-specific nuances. Consequently, the OEI quantifies how close any treatment group comes to this optimal physiological state.The Physiological Cost Index (PCI) was calculated to estimate the metabolic cost of osmoregulation: PCI = (Cortisol × 0.4) + (Ion_deviation × 0.6), where Ion_deviation = (Na_dev + K_dev + Cl_dev)/3. Stress Recovery Index (SRI) was calculated as SRI = (1 – (Cortisol_final – Cortisol_initial)/(Cortisol_peak – Cortisol_initial)) × 100, with higher values indicating better recovery. An Overall Health Index (OHI) was derived by combining OEI, SRI, and inverted PCI scores: OHI = (OEI × 0.4) + (SRI × 0.3) + ((100 – PCI) × 0.3). Optimal production conditions were determined by ranking treatments based on a composite score integrating ion regulation (60% weight) and stress response (40% weight).

These indices were developed as exploratory within-study summary metrics to facilitate comparison among treatments. They were not externally validated biomarkers and should be interpreted as relative ranking tools rather than absolute physiological endpoints. The weighting scheme was selected a priori to reflect the biological emphasis of this study on ionoregulatory status and stress response, but alternative weighting choices could produce different absolute scores. Accordingly, these indices were used only to summarize patterns already evident in the individual physiological, histological, and survival variables.

3. Results

3.1. Physiological indices

3.1.1. Three-way mixed model ANOVA

The three-way mixed-effects ANOVA revealed significant effects of salinity, weight class, time, and interactions on most physiological variables (Table 1). Na^+, Cl^-, cortisol, and Ca^{2+} showed significant main effects and interaction terms ($p < 0.001$), while K^+ was primarily influenced by weight class and time, with no significant effect of salinity ($p > 0.05$). The strongest temporal effect was observed for cortisol ($F_{6,224} = 1343.54$, $p < 0.001$), followed by Na^+ and K^+ (Table 1). (See Table 2.)

3.1.2. Cortisol response

Temporal analysis of cortisol levels revealed distinct size-dependent patterns across all time points (Fig. 2). In 0.5–1 g fish, cortisol levels remained relatively stable across early time points (9.2–12.1 ng/mL) but increased by 624 h, reaching 13.5–15.3 ng/mL. The highest cortisol in this size class was observed at 12 ppt (15.30 ± 0.12 ng/mL), followed by 8 ppt (14.55 ± 0.14 ng/mL) and 4 ppt (14.00 ± 0.06 ng/mL). In 1–3 g fish, cortisol levels showed an initial increase followed by a gradual change over time. At 3 h, levels were 9.6–11.2 ng/mL, peaking at 48 h (10.4–11.9 ng/mL) and reaching 14.1–14.9 ng/mL at 624 h. The highest cortisol in this size class was recorded at 12 ppt (14.90 ± 0.17 ng/mL) and 8 ppt (14.70 ± 0.12 ng/mL). The lowest cortisol levels were observed in 3–5 g fish maintained in freshwater (0 ppt: 12.55 ± 0.20 ng/mL), followed by 3–5 g fish at 8 ppt (12.60 ± 0.23 ng/mL) and 3–5 g fish at 12 ppt (12.85 ± 0.14 ng/mL). These three groups shared the same statistical grouping. In 3–5 g fish at 4 ppt, cortisol was 13.70 ± 0.12 ng/mL. In 5–10 g fish, cortisol levels ranged from 14.2 to 15.1 ng/mL at 624 h, with no significant differences among salinities. The lowest value in this size class was at 0 ppt (14.20 ± 0.17 ng/mL).

Table 2
Three-way mixed model ANOVA results for plasma osmolality in stellate sturgeon juveniles. Values are F-statistics with degrees of freedom (numerator, denominator). Significance levels: *** p < 0.001, ** p < 0.01, * p < 0.05, ns = not significant. Tank was included as a random factor in the model.

Effect	F-value (df)	*P*-value	Significance
Salinity	$F_{3,73} = 1.53$	0.215	ns
Weight Class	$F_{3,73} = 3.92$	0.012	*
Time	$F_{1,73} = 68.29$	<0.001	***
Salinity × Weight Class	$F_{9,73} = 3.16$	0.003	**
Salinity × Time	$F_{3,73} = 17.68$	<0.001	***
Weight Class × Time	$F_{3,73} = 8.05$	<0.001	***
Salinity × Weight Class × Time	$F_{9,73} = 2.45$	0.015	*

3.2. K^+ regulation

Temporal analysis of Na^+ levels revealed variation across size classes and time points (Fig. 3). In 0.5–1 g fish, Na^+ levels were 10.8–12.5 mmol/L at 3–12 h. Although levels increased over time, reaching 69.1–108.0 mmol/L at 624 h, they remained variable, with the lowest values at 0 ppt (69.1 ± 1.8 mmol/L) and the highest at 12 ppt (108.0 ± 1.1 mmol/L). In 1–3 g fish, Na^+ ranged from 24.8 to 82.6 mmol/L at 3 h, with the lowest at 0 ppt (24.8 ± 0.1 mmol/L) and the highest at 12 ppt (82.6 ± 0.6 mmol/L). By 624 h, Na^+ levels ranged from 85.9 to 116.3 mmol/L, with values of 106.4 ± 1.7 mmol/L at 8 ppt and 116.3 ± 0.6 mmol/L at 12 ppt. In 3–5 g fish, Na^+ levels ranged from 85.8 to 125.3 mmol/L across all time points. At 3 h, levels were 85.8–106.1 mmol/L. By 624 h, values were between 105.4 and 114.9 mmol/L, with 112.8 ± 2.2 mmol/L at 8 ppt and 106.5 ± 1.2 mmol/L at 0 ppt. In 5–10 g fish, Na^+ levels ranged from 87.6 to 116.8 mmol/L at 3 h. By 624 h, Na^+ levels were 93.9–109.7 mmol/L, with 99.7 ± 2.3 mmol/L at 8 ppt, 93.3 ± 3.0 mmol/L at 4 ppt, and 93.9 ± 2.0 mmol/L at 0 ppt.

3.2. K^+ regulation

Temporal analysis of K^+ levels revealed variation across size classes and time points (Fig. 4). In 0.5–1 g fish, K^+ levels were consistently elevated across all time points, ranging from 26.2 to 36.2 mmol/L at 624 h, with the highest values at 4 ppt (36.21 ± 1.26 mmol/L) and 12 ppt (36.09 ± 1.25 mmol/L). In 1–3 g fish, K^+ levels ranged from 26.7 to 33.2 mmol/L at 3 h, with the highest value at 12 ppt (33.19 ± 1.29 mmol/L). By 624 h, K^+ levels decreased to 2.6–4.5 mmol/L, with 4.45 ± 0.67 mmol/L at 8 ppt. In 3–5 g fish, K^+ levels ranged from 2.5 to 3.9 mmol/L across all time points. At 624 h, all values were between 2.6 and 3.4 mmol/L, with no significant differences among salinities. In 5–10 g fish, K^+ levels ranged from 2.1 to 7.2 mmol/L across all time points. At 624 h, K^+ levels were 2.9–7.2 mmol/L, with the lowest value at 12 ppt (2.94 ± 0.00 mmol/L) and the highest at 0 ppt (7.22 ± 0.53 mmol/L). All values at 624 h fell within the same statistical group.

3.3. Ca^{2+} and cl^- regulation

Ca^{2+} levels showed distinct patterns across weight classes (Fig. 5). In 0.5–1 g fish, Ca^{2+} remained between 9.2 and 10.6 mmol/L across all time points, with the lowest values at 624 h (9.70 ± 0.08 mmol/L at 0

Table 1
Three-way mixed model ANOVA summary for all physiological parameters in stellate sturgeon juveniles exposed to different salinities.

Parameter	Salinity	Weight Class	Time	Salinity × Weight	Salinity × Time	Weight × Time	Salinity × Weight × Time
Calcium	$F_{3,224} = 0.05$ ns	$F_{3,224} = 14.26$***	$F_{6,224} = 19.14$***	$F_{9,224} = 0.01$ ns	$F_{18,224} = 7.23$***	$F_{18,224} = 14.35$***	$F_{54,224} = 3.57$***
Sodium	$F_{3,224} = 87.85$***	$F_{3,224} = 189.03$***	$F_{6,224} = 500.94$***	$F_{9,224} = 5.37$***	$F_{18,224} = 26.16$***	$F_{18,224} = 172.57$***	$F_{54,224} = 10.67$***
Potassium	$F_{3,224} = 1.23$ ns	$F_{3,224} = 90.33$***	$F_{6,224} = 344.13$***	$F_{9,224} = 1.56$ ns	$F_{18,224} = 30.90$***	$F_{18,224} = 353.34$***	$F_{54,224} = 45.64$***
Chloride	$F_{3,224} = 9.73$***	$F_{3,224} = 282.09$***	$F_{6,224} = 45.76$***	$F_{9,224} = 27.18$***	$F_{18,224} = 5.89$***	$F_{18,224} = 23.31$***	$F_{54,224} = 3.92$***
Cortisol	$F_{3,224} = 8.17$***	$F_{3,224} = 141.79$***	$F_{6,224} = 1343.54$***	$F_{9,224} = 10.58$***	$F_{18,224} = 10.69$***	$F_{18,224} = 210.91$***	$F_{54,224} = 9.37$***

Note: Values show F-statistics with degrees of freedom (numerator, denominator). Significance levels: *** $p < 0.001$, ** $p < 0.01$, * $p < 0.05$, ns = not significant. Tank was included as a random factor in all models.

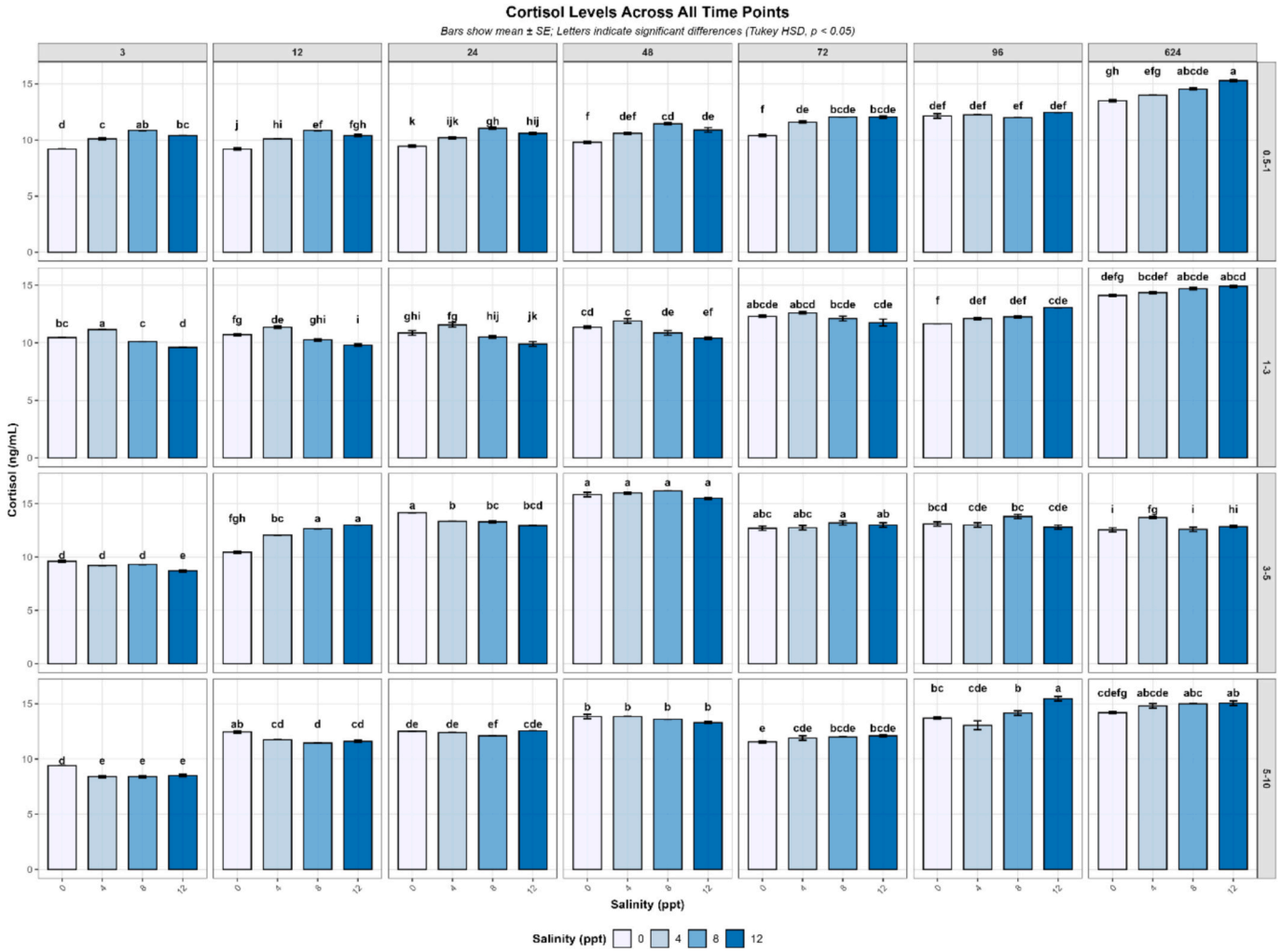

Fig. 2. Cortisol levels (ng/mL) in stellate sturgeon juveniles across all time points and weight classes. Bars represent mean cortisol concentrations ± standard error (SE). Fish were exposed to four salinities (0, 4, 8, 12 ppt) represented by a blue gradient from light blue (0 ppt) to dark blue (12 ppt). Data are presented for four weight classes: 0.5–1 g, 1–3 g, 3–5 g, and 5–10 g, across seven time points: 3, 12, 24, 48, 72, 96, and 624 h post-transfer. Different letters above bars indicate significant differences among treatments within each time point and weight class (Tukey HSD post-hoc test, $p < 0.05$). Bars sharing the same letter are not significantly different. (For interpretation of the references to colour in this figure legend, the reader is referred to the web version of this article.)

ppt) and the highest at 12 h (10.36 ± 0.34 mmol/L). In 1–3 g fish, Ca^{2+} ranged from 10.2 to 11.7 mmol/L, with no clear temporal trend. In 3–5 g and 5–10 g fish, Ca^{2+} increased from 11.2 to 11.7 mmol/L at 3 h to 12.1–12.7 mmol/L at 624 h. At 624 h, 3–5 g and 5–10 g fish showed the highest Ca^{2+} levels (12.1–12.7 mmol/L), with no significant differences among salinities within each weight class. Cl^- levels showed variation across weight classes and time points (Fig. 6). In 0.5–1 g fish, Cl^- remained at 95–115 mmol/L across most time points, with slightly higher values at 624 h (115–130 mmol/L). In 1–3 g fish, Cl^- ranged from 78.5 ± 0.9 mmol/L at 3 h to 139.0 ± 5.1 mmol/L at 624 h. In 3–5 g fish, Cl^- levels were 132.5–137.5 mmol/L at 12 h and 125–138 mmol/L at 624 h. In 5–10 g fish, Cl^- levels ranged from 110 to 136 mmol/L across all time points, with 110.5 ± 4.3 mmol/L at 0 ppt.

3.4. Plasma osmolality

Plasma osmolality in stellate sturgeon juveniles was significantly influenced by time, weight class, and the interactions between factors (three-way mixed model ANOVA, Table 3). Time exhibited the strongest effect ($F_{1,73} = 68.29$, $p < 0.001$), with osmolality increasing from initial (3 h) to final (624 h) sampling in all treatment combinations. Weight class also showed a significant effect ($F_{3,73} = 3.92$, $p < 0.05$). The significant two-way interactions (Salinity × Weight Class: $F_{9,73} = 3.16$, $p < 0.01$; Salinity × Time: $F_{3,73} = 17.68$, $p < 0.001$; Weight Class × Time: $F_{3,73} = 8.05$, $p < 0.001$) were observed across combinations of salinity, fish size, and exposure duration. The three-way interaction (Salinity × Weight Class × Time) was not estimable due to the experimental design.

At 3 h post-transfer, plasma osmolality ranged from 197 ± 17 mOsmol/L to 266 ± 5 mOsmol/L across treatments (Fig. 7). The lowest values were observed in 0.5–1 g fish maintained in freshwater (0 ppt: 197 ± 17 mOsmol/L), followed by 1–3 g fish in 4 ppt (219 ± 10 mOsmol/L) and 3–5 g fish in 8 ppt (239 ± 4 mOsmol/L). The highest initial osmolality was recorded in 5–10 g fish at 12 ppt (266 ± 5 mOsmol/L). These differences were statistically significant, with four distinct letter groupings among treatments. After 624 h of exposure, plasma osmolality ranged from 251 to 284 mOsmol/L across all treatments (Fig. 14). At 624 h, the mean osmolality values were 284 ± 15 mOsmol/L for 4 ppt in 1–3 g fish, 273 ± 15 mOsmol/L for 8 ppt in 3–5 g fish, 258 ± 18 mOsmol/L for 0 ppt in 0.5–1 g fish, and 251 ± 10 mOsmol/L for 12 ppt in 5–10 g fish. The temporal change from initial to final sampling ranged from 31 mOsmol/L (12 ppt, 5–10 g fish: 266 to 251 mOsmol/L) to 87 mOsmol/L (8 ppt, 3–5 g fish: 239 to 273 mOsmol/L).

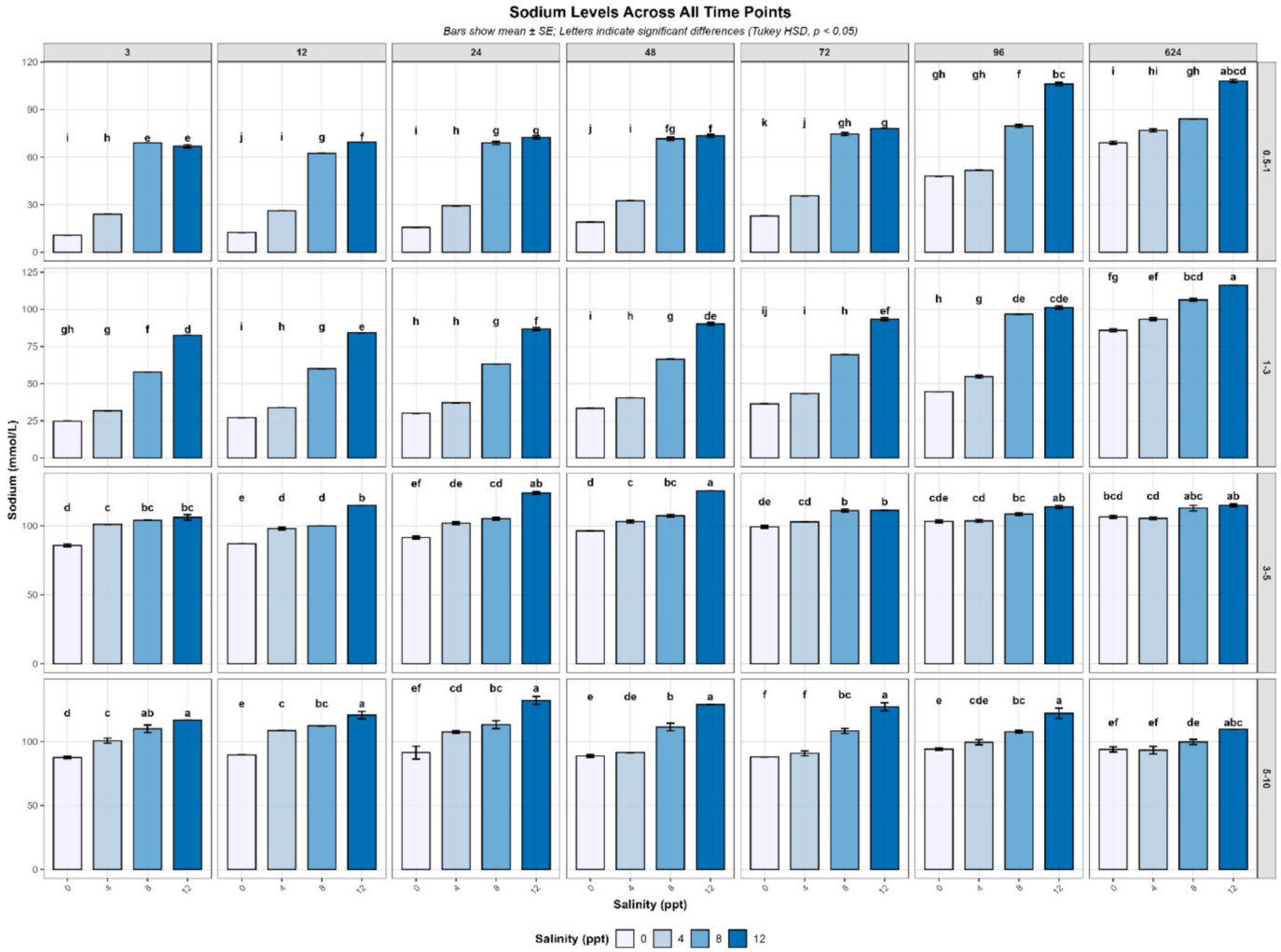

Fig. 3. Na^+ levels (mmol/L) in stellate sturgeon juveniles across all time points and weight classes. Bars represent mean Na^+ concentrations ± standard error (SE). Fish were exposed to four salinities (0, 4, 8, 12 ppt) represented by a blue gradient from light blue (0 ppt) to dark blue (12 ppt). Data are presented for four weight classes: 0.5–1 g, 1–3 g, 3–5 g, and 5–10 g, across seven time points: 3, 12, 24, 48, 72, 96, and 624 h post-transfer. Different letters above bars indicate significant differences among treatments within each time point and weight class (Tukey HSD post-hoc test, $p < 0.05$). Bars sharing the same letter are not significantly different. (For interpretation of the references to colour in this figure legend, the reader is referred to the web version of this article.)

3.5. Histological analysis

Histopathological changes in gill and kidney tissues were assessed using a semi-quantitative 0–4 scoring scale (0 = none, 1 = mild, 2 = moderate, 3 = marked, 4 = severe). To facilitate interpretation, an overall severity grade (mean of all lesion scores per treatment) was calculated and statistically analyzed using one-way ANOVA followed by Tukey HSD post-hoc tests with compact letter display (Table 3 for gill, Table 4 for kidney). Treatments sharing the same letter are not significantly different ($p \geq 0.05$).

Gill lesions (Table 3, Fig. 8): The overall severity was significantly influenced by treatment (ANOVA, $p < 0.001$). The highest overall severity scores were observed in the smallest juveniles (0.5–1 g) at 8 ppt (3.2 ± 0.1), characterized by severe adhesion, pronounced hyperplasia, and clubbing of secondary lamellae. Similarly, 1–3 g fish at 8 ppt and 12 ppt also showed marked to severe lesions (2.8–2.9). In contrast, the largest fish (5–10 g) exhibited only moderate overall severity (1.8–2.4), with freshwater controls showing the lowest scores (1.2 ± 0.1).

Kidney lesions (Table 4, Fig. 9): Renal tissue damage also varied significantly among treatments (ANOVA, $p < 0.001$). The most severe overall scores were recorded in 1–3 g fish at 0 and 4 ppt (2.3–2.4), driven by marked glomerular expansion, tubular obstruction, and lymphoid/hematopoietic proliferation. Moderate severity was observed in 0.5–1 g fish at 4 ppt (2.1 ± 0.1) and 3–5 g fish at 4 ppt (1.8 ± 0.1). The lowest severity was found in 5–10 g fish at 4 ppt (0.6 ± 0.1), which showed only mild lymphoid/hematopoietic proliferation with no other significant lesions.

These results demonstrate that both salinity and body size independently influence the degree of branchial and renal damage in juvenile stellate sturgeon. The smallest juveniles (0.5–3 g) are most susceptible to structural damage at moderate to high salinities (4–12 ppt), while larger fish (≥5 g) exhibit remarkable resilience, maintaining near-normal gill and kidney architecture even at elevated salinities. This pattern aligns with the physiological and osmoregulatory data, further supporting the critical size threshold of 3 g for salinity tolerance in this species.

3.6. Mortality

Mortality was significantly affected by both salinity and weight class, with a significant interaction between these factors as determined by a generalized linear mixed model (GLMM) with binomial error structure and logit link function, incorporating tank as a random factor (Salinity: $\chi^2 = 24.56$, df = 3, $p < 0.001$; Weight Class: $\chi^2 = 31.89$, df = 3, $p < 0.001$; Salinity × Weight Class: $\chi^2 = 8.93$, df = 9, $p < 0.001$). The lowest

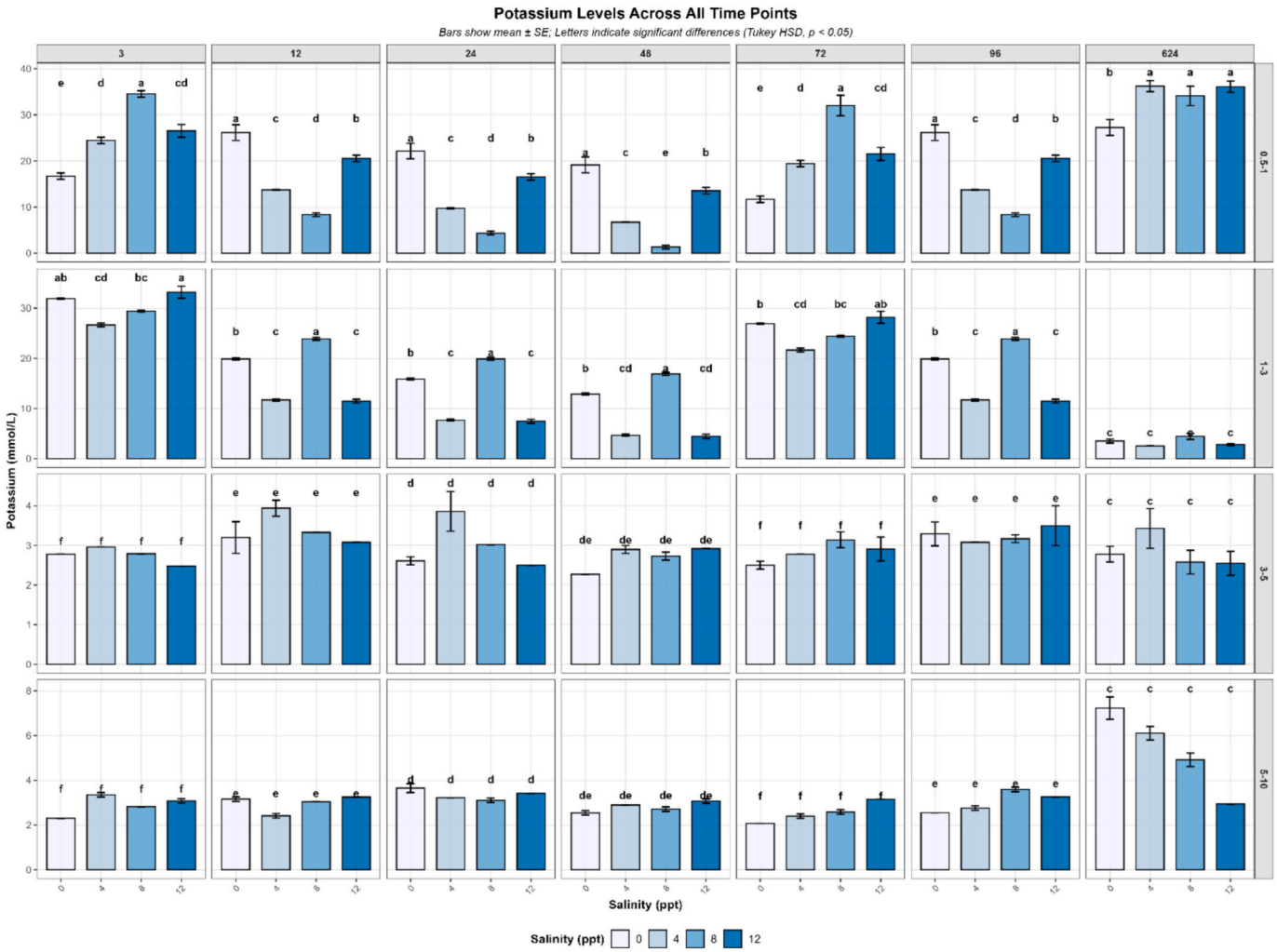

Fig. 4. K^+ levels (mmol/L) in stellate sturgeon juveniles across all time points and weight classes. Bars represent mean K^+ concentrations ± standard error (SE). Fish were exposed to four salinities (0, 4, 8, 12 ppt) represented by a blue gradient from light blue (0 ppt) to dark blue (12 ppt). Data are presented for four weight classes: 0.5–1 g, 1–3 g, 3–5 g, and 5–10 g, across seven time points: 3, 12, 24, 48, 72, 96, and 624 h post-transfer. Different letters above bars indicate significant differences among treatments within each time point and weight class (Tukey HSD post-hoc test, $p < 0.05$). Bars sharing the same letter are not significantly different. (For interpretation of the references to colour in this figure legend, the reader is referred to the web version of this article.)

predicted mortality rates from the GLMM (back-transformed to probability scale) were observed in 5–10 g fish across all salinities, ranging from 1.3% to 4.7% (Fig. 10), with the best survival at 4 ppt (1.3 ± 0.9%). The highest predicted mortality was recorded in 1–3 g fish at 12 ppt (27.3 ± 3.6%), followed by 0.5–1 g fish at 8 ppt (20.0 ± 3.3%) and 1–3 g fish at 4 ppt (18.0 ± 3.1%). All mortality values presented are back-transformed predicted probabilities from the GLMM with statistical letters indicating significant differences (Tukey-adjusted post-hoc comparisons, $p < 0.05$). Mortality values varied across size classes, with 5–10 g fish ranging from 1.3 to 4.7% across salinities, 3–5 g fish from 7.3 to 13.3%, 1–3 g fish from 9.3 to 27.3%, and 0.5–1 g fish from 4.7 to 20.0%. Fish >3 g (3–5 g and 5–10 g) showed mortality values of 1.3–13.3% across salinities, while fish <3 g (0.5–1 g and 1–3 g) showed higher mortality values at elevated salinities (>4 ppt, 16.0–27.3%). Mortality <5% occurred in 5–10 g fish at 0 ppt (2.7 ± 1.3%), 4 ppt (1.3 ± 0.9%), 8 ppt (3.3 ± 1.5%), and 12 ppt (4.7 ± 1.7%).

3.7. Composite indices and derived analyses

3.7.1. Exploratory composite indices

Based on a comprehensive scoring system integrating five physiological parameters (Ca^{2+}, Na^+, K^+, Cl^-, and cortisol) with 60% weight on ion regulation and 40% on stress response, adaptation scores were calculated for each treatment combination (Fig. 11). The highest score was observed in 0 ppt for 5–10 g fish (0.57). The next highest scores were 8 ppt for 5–10 g fish (0.56), 0 ppt for 3–5 g fish (0.56), 12 ppt for 3–5 g fish (0.55), and 4 ppt for 1–3 g fish (0.54). Scores for 5–10 g fish ranged from 0.56 to 0.57 at 0–8 ppt. Scores for 3–5 g fish ranged from 0.55 to 0.56 at 0–12 ppt. The score for 1–3 g fish at 4 ppt was 0.54. Scores for 0.5–1 g fish ranged from 0.22 to 0.32 across all salinities.

3.7.2. Allometric relationships

Correlation analysis revealed size-dependent patterns in ion regulation (Fig. 12). Na^+ showed positive correlations with body size across salinities ($r = 0.82$–0.91, $p < 0.001$). K^+ showed negative correlations with body size at 0 ppt ($r = -0.67$, $p < 0.01$) and 4 ppt ($r = -0.58$, $p < 0.05$). Na^+ and K^+ relationships were assessed across weight classes and salinity conditions. Correlation coefficients differed between ions and salinities as reported above.

3.7.3. Physiological stability across salinities

Analysis of coefficient of variation (CV) across salinities revealed size-dependent differences among physiological parameters (Fig. 13). The 5–10 g size class showed CV values of 6.2–15.7%. The 3–5 g class

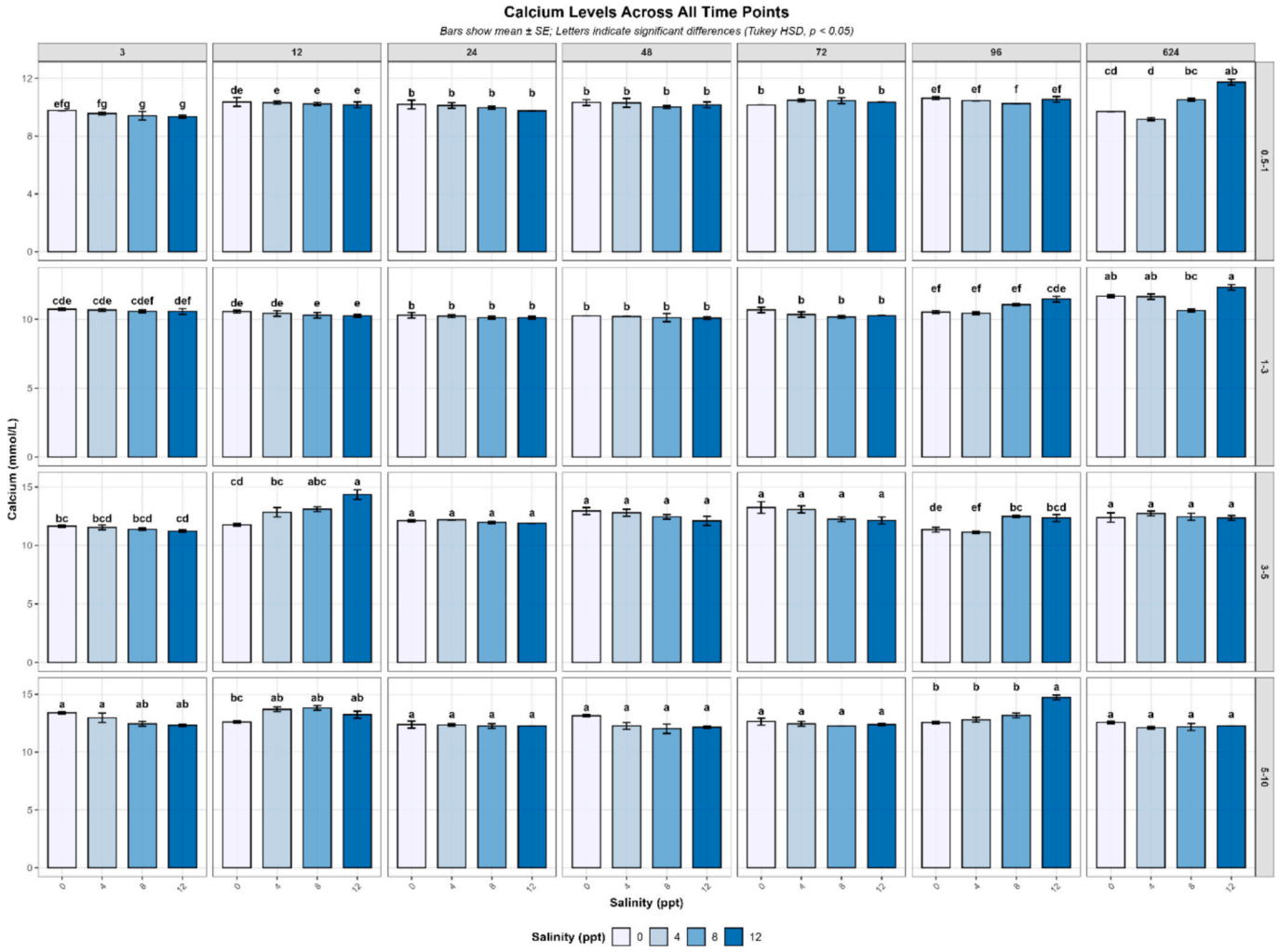

Fig. 5. Ca^{2+} levels (mmol/L) in stellate sturgeon juveniles across all time points and weight classes. Bars represent mean Ca^{2+} concentrations ± standard error (SE). Fish were exposed to four salinities (0, 4, 8, 12 ppt) represented by a blue gradient from light blue (0 ppt) to dark blue (12 ppt). Data are presented for four weight classes: 0.5–1 g, 1–3 g, 3–5 g, and 5–10 g, across seven time points: 3, 12, 24, 48, 72, 96, and 624 h post-transfer. Different letters above bars indicate significant differences among treatments within each time point and weight class (Tukey HSD post-hoc test, $p < 0.05$). Bars sharing the same letter are not significantly different. (For interpretation of the references to colour in this figure legend, the reader is referred to the web version of this article.)

showed CV values of 8.9–24.8%, the 1–3 g class showed 12.5–35.6%, and the 0.5–1 g class showed 15.8–67.3%. K^+ showed the highest CV values across size classes, while cortisol showed the lowest CV values across size classes.

3.7.4. Osmoregulatory efficiency index

The osmoregulatory efficiency index (OEI), combining Na/K and Na/Cl ratios, was calculated for all treatments (Fig. 14). The highest OEI values were observed in 5–10 g fish at 8 ppt (OEI = 87.3), followed by 5–10 g fish at 0 ppt (OEI = 82.1) and 3–5 g fish at 8 ppt (OEI = 79.5). The lowest OEI values were recorded in 0.5–1 g fish across all salinities (OEI = 12.4–45.6). OEI values ranged across size classes and salinities, with values above 70 observed in fish >3 g under certain conditions. *3.8.5. Physiological cost index.*

The Physiological Cost Index (PCI), integrating stress (cortisol) and ion deviation, was calculated for all treatments (Fig. 15). The lowest PCI was found in 5–10 g fish at 0 ppt (PCI = 24.3), followed by 3–5 g fish at 0 ppt (PCI = 26.7) and 5–10 g fish at 8 ppt (PCI = 28.1). The highest PCI was recorded in 0.5–1 g fish at 12 ppt (PCI = 68.4). PCI values ranged from 24.3 to 68.4 across treatments. In fish >3 g, PCI values were below 40 in several treatments. *3.8.6. Stress recovery dynamics.*

Analysis of cortisol dynamics revealed size-dependent recovery patterns (Fig. 16). Larger fish (5–10 g) showed cortisol levels returning to near-baseline values by 96 h, with a reported 92.3% recovery. Medium-sized fish (3–5 g) showed 78.5% recovery by 96 h, while small fish (0.5–1 g) showed 45.2% recovery at 96 h and remained elevated up to 624 h. The 1–3 g fish showed 62.5% recovery by 624 h.

4. Discussion

The present study shows that juvenile stellate sturgeon responds to salinity exposure through a coordinated but strongly size-dependent suite of physiological and histological changes. The most consistent systemic responses were observed in Na^+, cortisol, and plasma osmolality, while K^+ exhibited a more size- and time-specific pattern, and Ca^{2+} was comparatively stable. Together, these results indicate that salinity challenge in this species is not expressed as a uniform disturbance across all blood parameters, but rather as an integrated osmoregulatory response in which Na^+ and cortisol are the most sensitive indicators of physiological adjustment. For example, Atlantic sturgeon transferred to 25% salinity shows transient spikes in plasma Cl^- and cortisol, markers of osmotic stress (McCormick et al., 2020), and cortisol is known to promote seawater acclimation by upregulating gill ion transport mechanisms. This interpretation is consistent with general fish

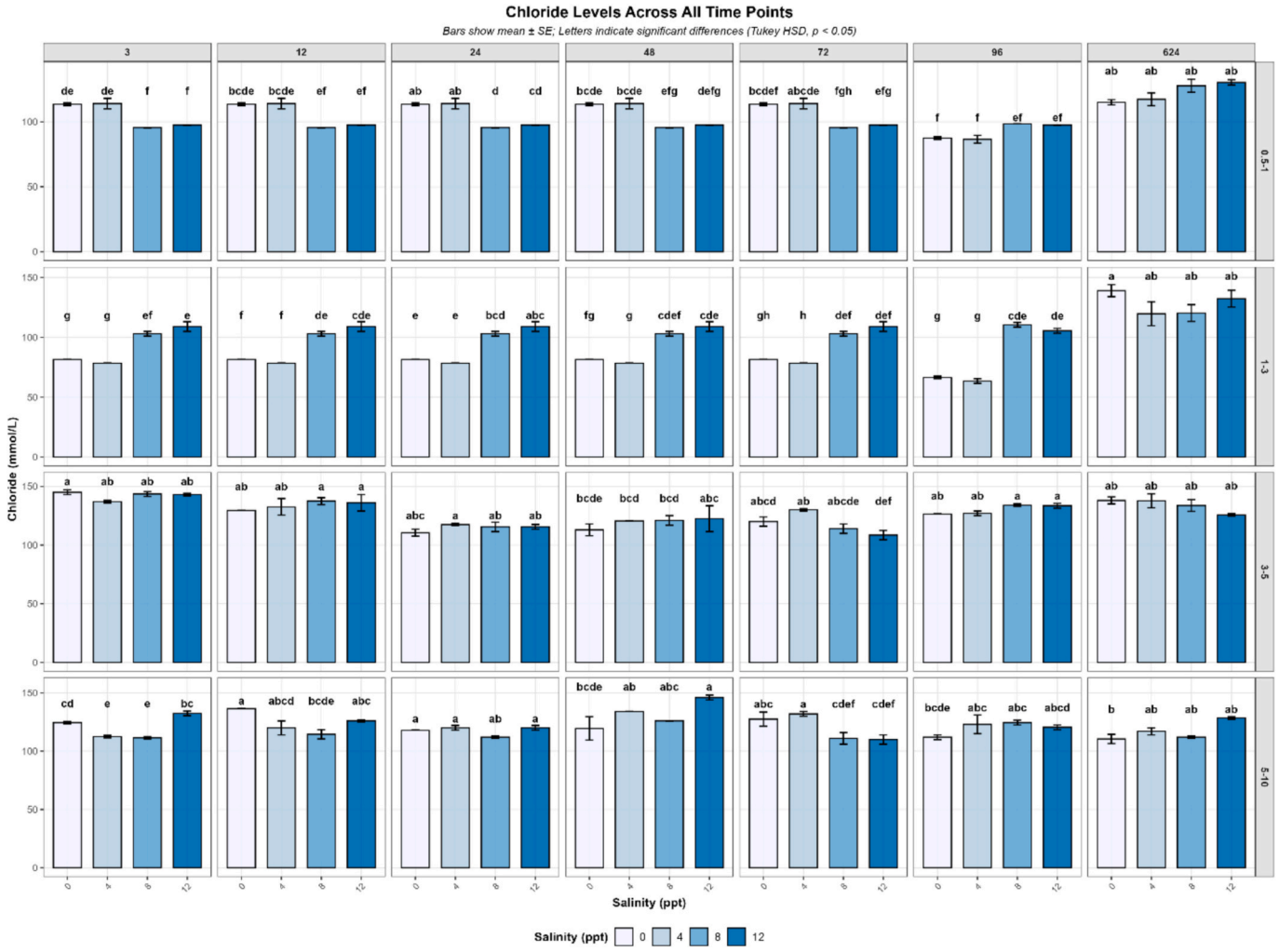

Fig. 6. Cl^- levels (mmol/L) in stellate sturgeon juveniles across all time points and weight classes. Bars represent mean Cl^- concentrations ± standard error (SE). Fish were exposed to four salinities (0, 4, 8, 12 ppt) represented by a blue gradient from light blue (0 ppt) to dark blue (12 ppt). Data are presented for four weight classes: 0.5–1 g, 1–3 g, 3–5 g, and 5–10 g, across seven time points: 3, 12, 24, 48, 72, 96, and 624 h post-transfer. Different letters above bars indicate significant differences among treatments within each time point and weight class (Tukey HSD post-hoc test, $p < 0.05$). Bars sharing the same letter are not significantly different. (For interpretation of the references to colour in this figure legend, the reader is referred to the web version of this article.)

Table 3
Mean semi-quantitative scores (0–4) for gill lesions in juvenile *Acipenser stellatus* exposed to different salinities across four weight classes. Scores were based on coded hematoxylin and eosin–stained sections, where 0 = none and 4 = severe. Values are mean ± SD. Different letters indicate significant differences among treatments ($p < 0.05$). Representative micrographs are shown in Fig. 8.

Weight class (g)	Salinity (ppt)	Adhesion	Hyperplasia	Necrosis	Congestion	Hemorrhage	Epithelial damage	Clubbing	Hemosiderin
0.5–1	0	0.8 ± 0.4d	0.8 ± 0.4c	0.8 ± 0.4d	0.8 ± 0.4d	0.0 ± 0.0e	0.8 ± 0.4d	0.0 ± 0.0e	0.0 ± 0.0d
0.5–1	4	0.8 ± 0.4d	0.8 ± 0.4c	0.8 ± 0.4d	2.8 ± 0.4b	0.8 ± 0.4d	0.0 ± 0.0e	0.0 ± 0.0e	0.8 ± 0.4c
0.5–1	8	3.8 ± 0.4a	2.8 ± 0.4a	0.8 ± 0.4d	1.8 ± 0.4c	1.8 ± 0.4c	0.8 ± 0.4d	2.8 ± 0.4b	0.0 ± 0.0d
0.5–1	12	3.8 ± 0.4a	1.8 ± 0.4b	0.8 ± 0.4d	0.8 ± 0.4d	0.8 ± 0.4d	1.8 ± 0.4c	0.0 ± 0.0e	1.8 ± 0.4b
1–3	0	1.8 ± 0.4c	0.8 ± 0.4c	0.8 ± 0.4d	3.8 ± 0.4a	2.8 ± 0.4b	1.8 ± 0.4c	0.0 ± 0.0e	0.0 ± 0.0d
1–3	4	2.8 ± 0.4b	2.8 ± 0.4a	1.8 ± 0.4c	2.8 ± 0.4b	2.8 ± 0.4b	1.8 ± 0.4c	0.8 ± 0.4d	0.8 ± 0.4c
1–3	8	3.7 ± 0.5a	2.7 ± 0.5a	3.7 ± 0.5a	2.7 ± 0.5b	2.7 ± 0.5b	3.7 ± 0.5a	0.7 ± 0.5d	0.0 ± 0.0d
1–3	12	3.7 ± 0.5a	1.7 ± 0.5b	3.7 ± 0.5a	1.7 ± 0.5c	1.7 ± 0.5c	2.7 ± 0.5b	0.0 ± 0.0e	0.7 ± 0.5c
3–5	0	1.8 ± 0.4c	0.8 ± 0.4c	0.8 ± 0.4d	2.8 ± 0.4b	2.8 ± 0.4b	0.8 ± 0.4d	1.8 ± 0.4c	0.8 ± 0.4c
3–5	4	2.8 ± 0.4b	1.8 ± 0.4b	2.8 ± 0.4b	3.8 ± 0.4a	2.8 ± 0.4b	2.8 ± 0.4b	0.8 ± 0.4d	0.0 ± 0.0d
3–5	8	3.8 ± 0.4a	0.8 ± 0.4c	2.8 ± 0.4b	2.8 ± 0.4b	2.8 ± 0.4b	3.8 ± 0.4a	0.8 ± 0.4d	0.0 ± 0.0d
3–5	12	2.8 ± 0.4b	2.8 ± 0.4a	1.8 ± 0.4c	2.8 ± 0.4b	2.8 ± 0.4b	2.8 ± 0.4b	0.8 ± 0.4d	0.0 ± 0.0d
5–10	0	0.8 ± 0.4d	0.8 ± 0.4c	3.8 ± 0.4a	3.8 ± 0.4a	2.8 ± 0.4b	3.8 ± 0.4a	2.8 ± 0.4b	0.0 ± 0.0d
5–10	4	2.8 ± 0.4b	1.8 ± 0.4b	2.8 ± 0.4b	3.8 ± 0.4a	3.8 ± 0.4a	3.8 ± 0.4a	0.8 ± 0.4d	0.0 ± 0.0d
5–10	8	2.8 ± 0.4b	0.8 ± 0.4c	3.8 ± 0.4a	2.8 ± 0.4b	2.8 ± 0.4b	3.8 ± 0.4a	0.0 ± 0.0e	0.0 ± 0.0d
5–10	12	3.8 ± 0.4a	2.8 ± 0.4a	2.8 ± 0.4b	3.8 ± 0.4a	2.8 ± 0.4b	2.8 ± 0.4b	3.8 ± 0.4a	2.8 ± 0.4a

osmoregulatory physiology, in which salinity elevation increases the osmotic gradient between the external medium and body fluids and therefore activates endocrine and ion-transport responses to stabilize homeostasis (McCormick et al., 2020). In many euryhaline fishes,

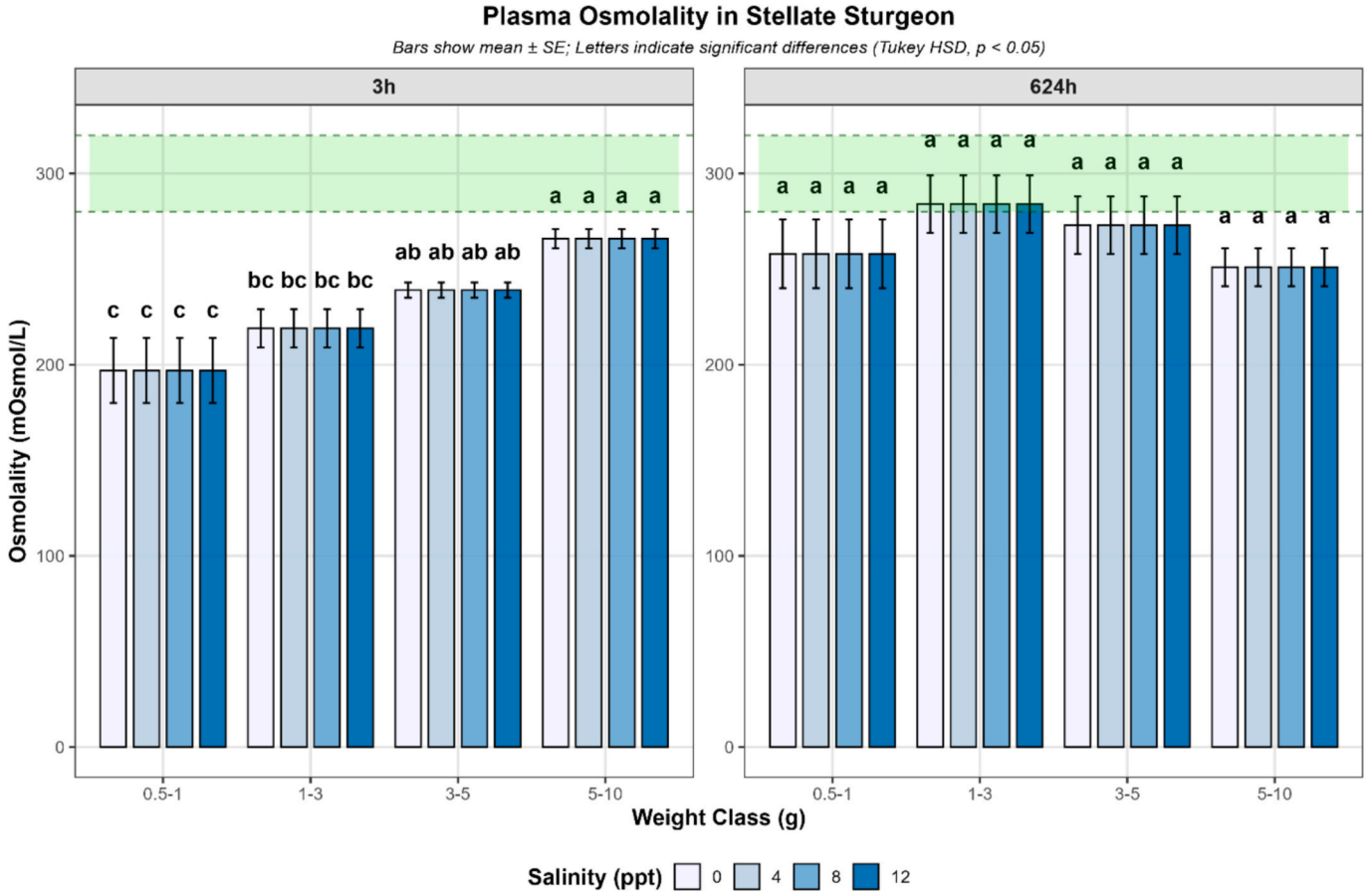

Fig. 7. Plasma osmolality in stellate sturgeon juveniles. Bars represent mean osmolality ± standard error (SE). Fish were exposed to four salinities (0, 4, 8, 12 ppt) represented by a blue gradient from light blue (0 ppt) to dark blue (12 ppt), consistent with the colour scheme used throughout this study. Data are presented for four weight classes: 0.5–1 g, 1–3 g, 3–5 g, and 5–10 g at 3 h (initial response) and 624 h (final adaptation). Different letters above bars indicate significant differences among treatments within each time point (Tukey HSD post-hoc test, $p < 0.05$). Bars sharing the same letter are not significantly different. (For interpretation of the references to colour in this figure legend, the reader is referred to the web version of this article.)

Table 4
Mean semi-quantitative scores (0–4) for kidney lesions in juvenile *Acipenser stellatus* exposed to different salinities across four weight classes. Scores were based on coded hematoxylin and eosin–stained sections, where 0 = none and 4 = severe. Values are mean ± SD. Different letters indicate significant differences among treatments ($p < 0.05$). Representative micrographs are shown in Fig. 9.

Weight class (g)	Salinity (ppt)	Glomerular expansion	Tubular obstruction	Tubular necrosis	Hypertrophy	Congestion	Hemorrhage	Lymphoid/ hematopoietic tissue	Hemosiderin
0.5–1	0	2.8 ± 0.4a	0.0 ± 0.0b	1.8 ± 0.4b	0.0 ± 0.0b	0.8 ± 0.4c	0.8 ± 0.4c	0.0 ± 0.0c	0.0 ± 0.0c
0.5–1	4	2.8 ± 0.4a	2.8 ± 0.4a	1.8 ± 0.4b	2.8 ± 0.4a	1.8 ± 0.4b	1.8 ± 0.4b	2.8 ± 0.4a	1.8 ± 0.4a
1–3	0	2.8 ± 0.4a	0.0 ± 0.0b	2.8 ± 0.4a	2.8 ± 0.4a	2.8 ± 0.4a	2.8 ± 0.4a	2.8 ± 0.4a	0.0 ± 0.0c
1–3	4	2.8 ± 0.4a	2.8 ± 0.4a	1.8 ± 0.4b	2.8 ± 0.4a	2.8 ± 0.4a	2.8 ± 0.4a	2.8 ± 0.4a	0.0 ± 0.0c
1–3	8	2.7 ± 0.5a	0.0 ± 0.0b	1.7 ± 0.5b	0.0 ± 0.0b	0.7 ± 0.5c	0.7 ± 0.5c	2.7 ± 0.5a	0.0 ± 0.0c
3–5	4	0.0 ± 0.0b	2.8 ± 0.4a	1.8 ± 0.4b	2.8 ± 0.4a	1.8 ± 0.4b	1.8 ± 0.4b	1.8 ± 0.4b	0.8 ± 0.4b
5–10	0	2.8 ± 0.4a	0.0 ± 0.0b	1.8 ± 0.4b	0.0 ± 0.0b	2.8 ± 0.4a	2.8 ± 0.4a	0.0 ± 0.0c	1.8 ± 0.4a
5–10	4	0.0 ± 0.0b	0.0 ± 0.0b	0.0 ± 0.0c	0.0 ± 0.0b	0.0 ± 0.0d	0.0 ± 0.0d	2.6 ± 0.5a	0.0 ± 0.0c

plasma osmolality rises initially after transfer to higher salinity and then partially recovers as branchial and kidney transport systems adapt, a pattern also evident here, where plasma osmolality increased over time but converged within a narrower range by 624 h. These size-dependent responses are consistent with previous sturgeon studies showing that salinity tolerance and osmoregulatory capacity increase with growth. In juvenile Russian sturgeon, survival and ion regulation improved with age and size, with effective regulation reported above about 2.8 g; in Persian sturgeon, fish under 3 g were unable to survive elevated salinity, whereas larger juveniles acclimated more successfully. Green sturgeon also show age/size-dependent osmoregulatory performance in saline environments, supporting the interpretation that developmental maturation underlies the present size effect (Allen and Cech Jr, 2007; Farabi et al., 2011; Shirangi et al., 2016).

Our primary finding of a ~ 16% increase in plasma osmolality (from ~230 to ~266 mOsm·kg^{-1} over 624 h) reflects the classic osmoregulatory response of euryhaline fish to hyperosmotic environments. Salinity elevation increases the osmotic gradient between external water and internal fluids, compelling fish to adjust via active ion transport, water movement, and endocrine modulation (e.g., cortisol; McCormick et al., 2020). Teleost fishes typically regulate plasma osmolality around 260–380 mOsm·kg^{-1} (Evans and Claiborne, 2009; Thibaut et al., 2019; Lee et al., 2022), so our final osmolality (~266 mOsm·kg^{-1}) remains within the normal physiological range. In many euryhaline teleosts,

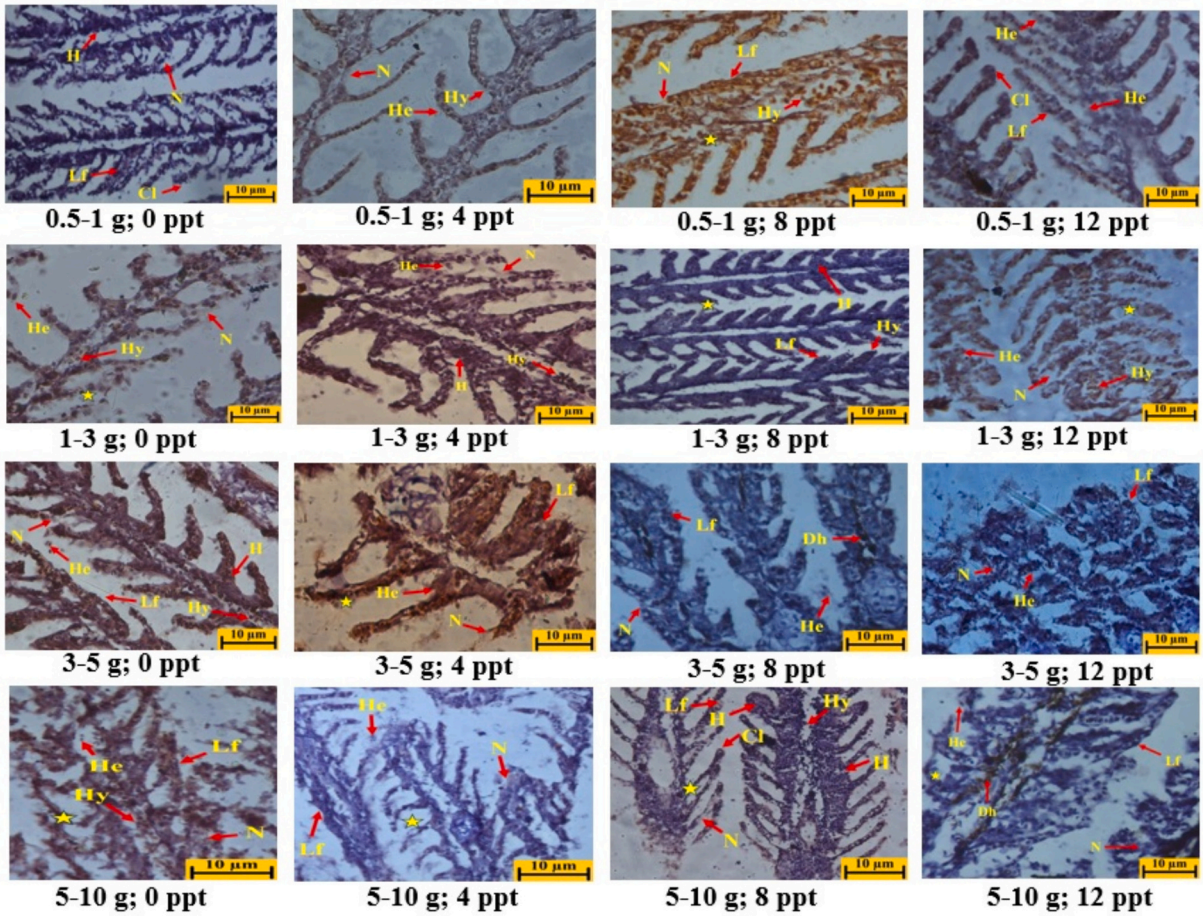

Fig. 8. Gill histopathology in stellate sturgeon juveniles. Representative hematoxylin and eosin-stained gill sections showing salinity- and size-dependent branchial lesions across four salinities (0, 4, 8, 12 ppt) and four weight classes (0.5–1, 1–3, 3–5, 5–10 g). Observed histopathological alterations include lamellar fusion (Lf), necrosis (N), hyperplasia (H), hyperemia (Hy), hemorrhage (He), clubbing of secondary lamellae (Cl), and hemosiderin deposition (Dh). Scale bar = 10 μm.

plasma osmolality rises during early exposure to increased salinity, followed by partial recovery as ion transporters and tissue adjustments compensate for the osmotic challenge (McCormick et al., 2020); our data mirror this pattern of an acute rise followed by stabilization. For example, Atlantic sturgeon exposed to 25‰ SW showed transient increases in plasma Cl^- and cortisol, which then subsided as gill transport proteins (e.g. NKCC) increased in abundance (McCormick et al., 2020).

The significant effects of salinity, weight class, and time on Na^+ are consistent with the central role of NaCl in fish osmotic homeostasis and with the need for coordinated gill and kidney responses during salinity acclimation. In euryhaline fishes, salinity challenge triggers dynamic changes in ion transport, water balance, and epithelial permeability, with NaCl regulation remaining a core component of extracellular osmotic control (Gonzalez, 2012; Kültz, 2015; Shirangi et al., 2016). In sturgeons, previous studies have shown that salinity transfer induces chloride-cell proliferation and increases gill Na^+/K^+-ATPase activity, and that juveniles above approximately 2 g have greater ion-transport capacity than smaller fish during freshwater-to-brackish transfer (Shirangi et al., 2016). The present results are consistent with these findings: the smallest juveniles showed the largest early Na^+ deviations, whereas fish >3 g maintained comparatively stable plasma Na^+ concentrations across salinities and time. Cl^- followed the same overall pattern as Na^+, consistent with its companion role in extracellular osmoregulation (Kültz, 2015; Shirangi et al., 2016). The Na^+–Cl^- pattern is also consistent with previous brackish-water studies in sturgeons and other teleosts showing that extracellular NaCl is the primary osmotic driver and that Na^+, K^+, Ca^{2+}, and Mg^{2+} commonly change during early salinity transfer before stabilising during acclimation (LeBreton and Beamish, 1998; Rodriguez et al., 2002; He et al., 2009).

K^+ showed a different pattern from Na^+ and Cl^-. Because K^+ is predominantly an intracellular ion and is tightly linked to Na^+/K^+-ATPase-mediated maintenance of membrane potential and intracellular ionic homeostasis, its plasma concentration is generally less directly coupled to external salinity than that of Na^+ and Cl^- (Gonzalez, 2012; Kültz, 2015; Takvam et al., 2021). In the present study, the smallest juveniles showed the highest early K^+ concentrations, whereas fish >3 g maintained values closer to the physiological range at later sampling points. Similar salinity-linked changes in plasma K^+ and other ions have been reported in juvenile sturgeons during brackish-water adaptation, including Chinese sturgeon, where plasma Na^+, K^+, Ca^{2+}, and Mg^{2+} increase under brackish conditions before stabilization, and juvenile green sturgeon, where larger size classes exhibit greater osmoregulatory capacity in saline environments (Allen and Cech Jr, 2007; He et al., 2009). These findings are consistent with our results and support the interpretation that body size strongly modulates K^+ regulation during salinity exposure, with smaller juveniles exhibiting less developed ionoregulatory control than larger fish (Allen and Cech Jr, 2007; He et al., 2009). The marked K^+ elevation in the smallest juveniles likely reflects immature intracellular ion regulation and limited Na^+/K^+-ATPase control, whereas the near-physiological values in fish above 3 g are consistent with the maturation of osmoregulatory capacity reported in older and larger sturgeons (Allen and Cech Jr, 2007; Farabi et al., 2011; Shirangi et al., 2016).

Ca^{2+} was less responsive to salinity than Na^+, which is physiologically plausible. Ca^{2+} in fish blood is under tighter endocrine and skeletal control than Na^+ or Cl^-, so short-term shifts in salinity tend to have

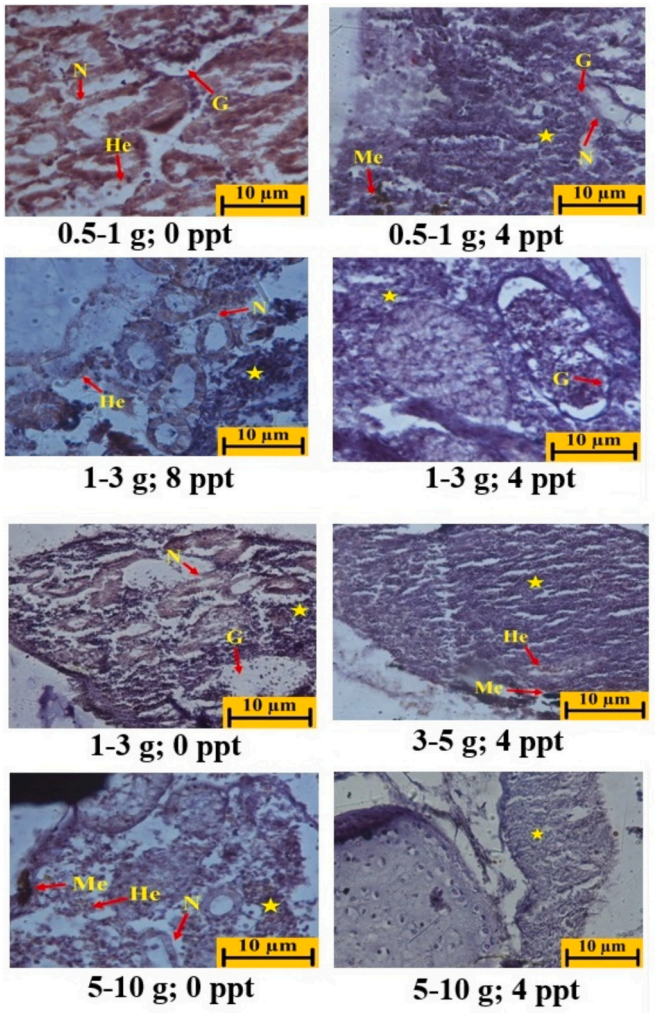

Fig. 9. Kidney histopathology in stellate sturgeon juveniles. Representative hematoxylin and eosin-stained kidney sections showing salinity- and size-dependent kidney lesions across four salinities (0, 4, 8, 12 ppt) and four weight classes (0.5–1, 1–3, 3–5, 5–10 g). Observed histopathological alterations include glomerular alteration (G; dilation, lumen obstruction, or loss of capillary network), necrosis (N), hemorrhage (He), melanomacrophage centres (Me), and leukocyte infiltration or head kidney hematopoietic tissue (*). Scale bar = 10 µm.

smaller effects on plasma Ca^{2+} (Gonzalez, 2012; Kültz, 2015). In our data, plasma Ca^{2+} changes were more strongly associated with weight class and time, likely reflecting growth-related processes such as skeletal mineralization, than with salinity per se. The relatively weak salinity effect on Ca^{2+} indicates that while Ca^{2+} measurements can complement other indices, they are not the most sensitive standalone indicator of acute osmotic stress in juvenile *A. stellatus*. Ca^{2+} changed less than the major monovalent ions and appeared to vary more with size and time than with salinity, consistent with tighter skeletal and endocrine control.

Cortisol showed the clearest temporal response and was the most dynamic stress-related variable. The overall pattern – a rapid rise in cortisol under salinity challenge followed by a decline in larger juveniles – is consistent with the canonical endocrine stress response in fish. Cortisol is the primary corticosteroid in teleosts and chondrosteans, and it actively promotes acclimation to hyperosmotic conditions by enhancing ion-transport capacity in gill and kidney epithelia (e.g., upregulating Na^+/K^+-ATPase and $Na^+/K^+/2Cl^-$ cotransporter; McCormick, 2011; McCormick et al., 2020). Its role is not limited to acute stress: cortisol also interacts with other hormones (e.g. growth hormone, prolactin) to fine-tune osmoregulatory performance during acclimation (McCormick, 2011). In this study, the smallest fish maintained elevated cortisol for much longer, indicating a prolonged stress load and slower recovery. In contrast, 3–5 g and 5–10 g fish recovered toward baseline more quickly, consistent with their more mature endocrine and transport systems. Importantly, prolonged cortisol elevation in the smaller juveniles may have been both a response to osmotic disturbance and a contributing factor to tissue injury. Although short-term cortisol secretion is adaptive, chronic elevation can increase metabolic demand, reduce cellular repair capacity, impair epithelial barrier integrity, and suppress immune and antioxidant functions (Wendelaar Bonga, 1997; Barton, 2002). These effects may help explain why the smallest fish, which showed sustained cortisol elevation, also exhibited more severe gill lesions (lamellar adhesion, epithelial lifting, necrosis, hemorrhage) and kidney pathology (glomerular deformation, tubular degeneration, congestion, hemosiderin accumulation). Thus, the endocrine and histological data together suggest that delayed cortisol recovery in smaller juveniles may amplify structural damage and prolong physiological instability under salinity stress. The stress data therefore reinforce the conclusion that body size strongly determines the capacity to cope with salinity exposure. The slower cortisol recovery in the smallest juveniles is also consistent with their weaker ionoregulatory performance, because prolonged endocrine stress can delay acclimation and increase metabolic costs. In euryhaline sturgeons, size- and age-related gains in salinity tolerance are commonly accompanied by faster recovery from osmotic challenges (Allen and Cech Jr, 2007; Farabi et al., 2011; Shirangi et al., 2016).

The plasma osmolality results provide additional support for the size-dependent interpretation. Although osmolality increased with exposure duration, all groups converged to a relatively restricted range by the final sampling, demonstrating that juveniles achieved partial physiological compensation. This fits the standard model of salinity acclimation: an early osmotic disturbance is followed by stabilization as transport systems, endocrine signalling, and tissue adjustments compensate (Kültz, 2015; McCormick et al., 2020). Importantly, the most stable and energetically efficient conditions were not necessarily identical across all indices. Our composite performance metrics and survival data indicate that the largest juveniles (5–10 g) consistently performed best overall, even though some intermediate sizes had favorable values for individual metrics. The composite indices (OEI, PCI, SRI, and OHI) broadly supported the univariate analyses, with larger juveniles generally ranking better than smaller juveniles under the tested conditions. This implies that release or transfer recommendations should be based on multiple indicators and survival outcomes, not a single parameter. The final osmolality values should be interpreted relative to the species range reported in the Introduction (approximately 250–270 mOsm kg^{-1}) rather than as evidence that 300 mOsm kg^{-1} is an optimal physiological set point. In this study, 300 mOsm kg^{-1} was not used as a biological optimum; instead, interpretation is based on the direction and magnitude of change across treatments and comparison with the published sturgeon range.

The histological findings in the gills show that salinity exposure caused size- and treatment-dependent branchial lesions. Gills are especially vulnerable because they are the primary respiratory surface and a major osmoregulatory interface (Dawood et al., 2022; Alsafy et al., 2025). We observed hyperplasia, lamellar adhesion, epithelial detachment, necrosis and hemorrhage in a graded manner, consistent with classic reports of gill pathology under osmotic stress. Hyperplasia and lamellar fusion can initially be adaptive barriers to passive ion flux but later compromise respiration (Ali et al., 2024). In this study, smaller juveniles developed more severe gill pathology at moderate salinities, consistent with their limited ionoregulatory capacity and immature epithelial defenses. Larger juveniles also showed substantial branchial damage, including severe lesions even in freshwater, suggesting that they may have had pre-existing stress or vulnerability (Singh, 2018). Similar gill remodelling (chloride-cell changes and tissue disruption) under salinity stress has been reported in other fish species (Fiol et al.,

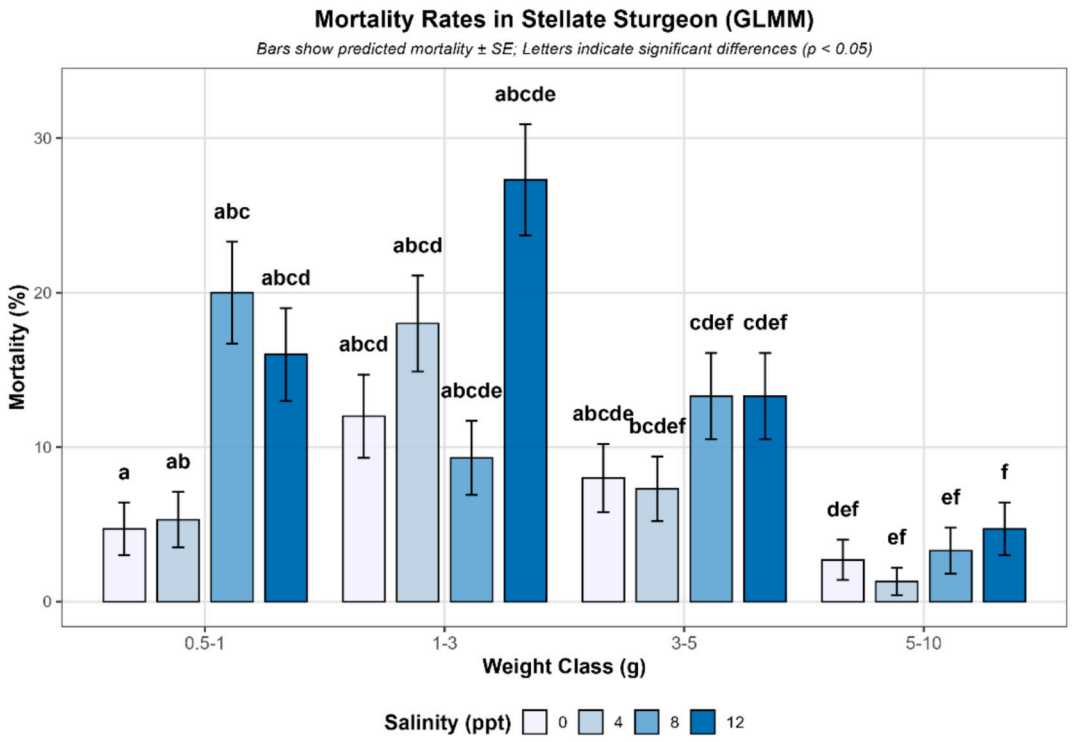

Fig. 10. Mortality rates (%) in stellate sturgeon juveniles across different salinities and weight classes. Bars represent mean mortality percentages ± standard error (SE). Fish were exposed to four salinities (0, 4, 8, 12 ppt) represented by a blue gradient from light blue (0 ppt) to dark blue (12 ppt), consistent with the colour scheme used for all physiological parameters. Data is presented for four weight classes: (A) 0.5–1 g, (B) 1–3 g, (C) 3–5 g, and (D) 5–10 g. Mortality was recorded over the entire 624-h experimental period. Different letters above bars indicate significant differences among treatments (Tukey HSD post-hoc test, $p < 0.05$). Bars sharing the same letter are not significantly different. (For interpretation of the references to colour in this figure legend, the reader is referred to the web version of this article.)

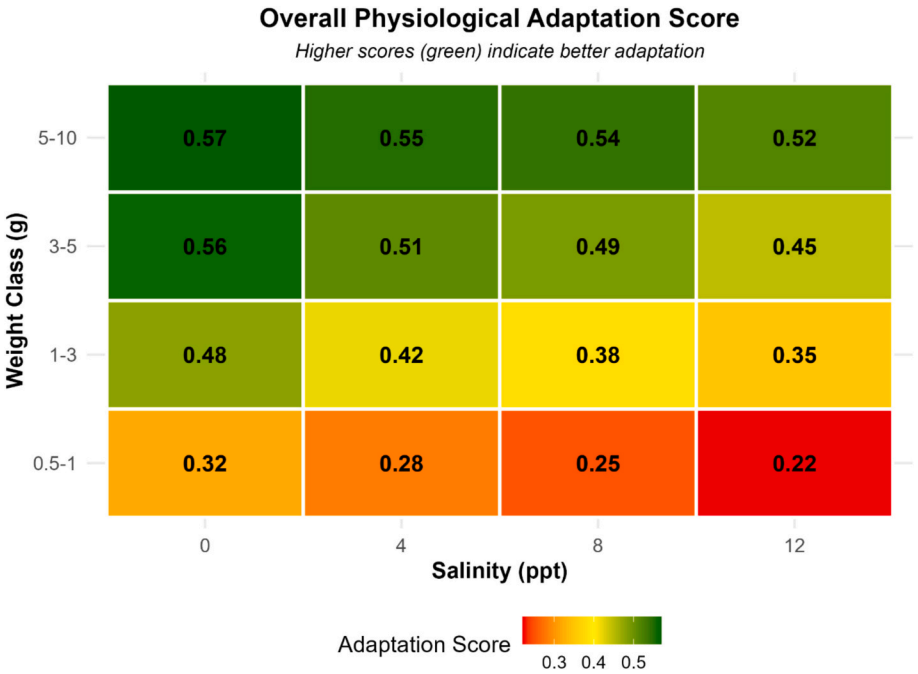

Fig. 11. Heatmap of overall physiological adaptation scores for stellate sturgeon juveniles exposed to four salinities (0, 4, 8, 12 ppt) across four weight classes (0.5–1, 1–3, 3–5, 5–10 g) at 624 h post-transfer. The overall adaptation score integrates all five physiological parameters (Ca^{2+}, Na^{+}, K^{+}, Cl^{-}, and Cortisol) with 60% weight on ion regulation and 40% on stress response. Higher scores (green) indicate better overall physiological adaptation, while lower scores (red) indicate poorer adaptation. Numbers within cells represent the mean adaptation score for each treatment combination. Colour scale: Green = Excellent adaptation (score > 0.50), Yellow = Moderate adaptation (score 0.35–0.50), Red = Poor adaptation (score < 0.35). (For interpretation of the references to colour in this figure legend, the reader is referred to the web version of this article.)

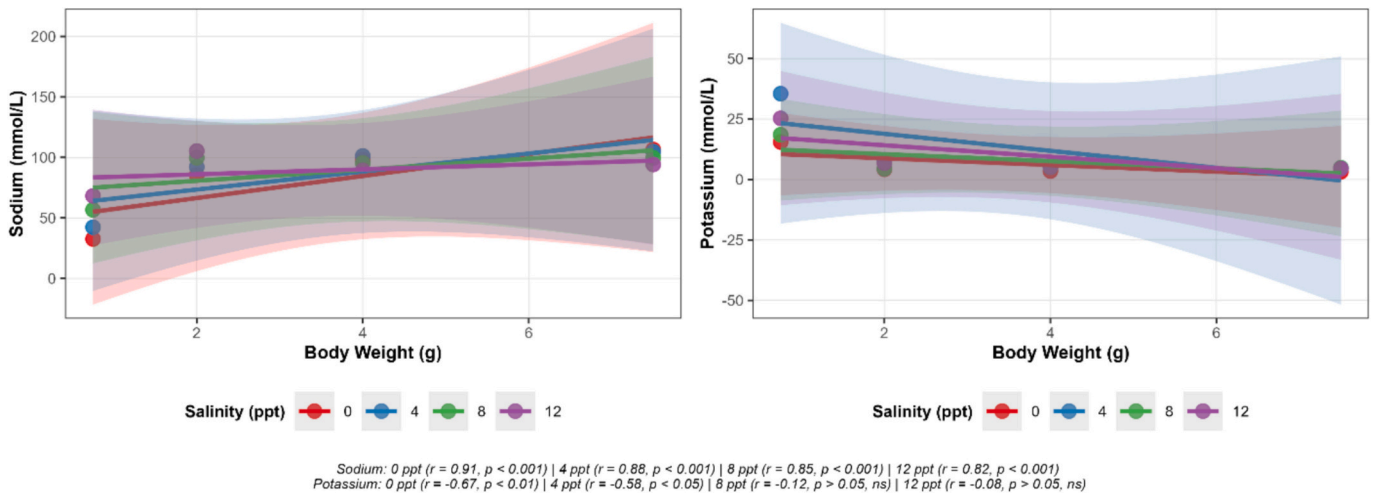

Fig. 12. Allometric relationships between body size and ion regulation in stellate sturgeon juveniles. Na^+ levels (mmol/L) as a function of body weight across four salinities (0, 4, 8, 12 ppt). Points represent mean Na^+ concentrations ($n = 3$ per treatment), lines show linear regression fits with 95% confidence intervals. K^+ levels (mmol/L) as a function of body weight.

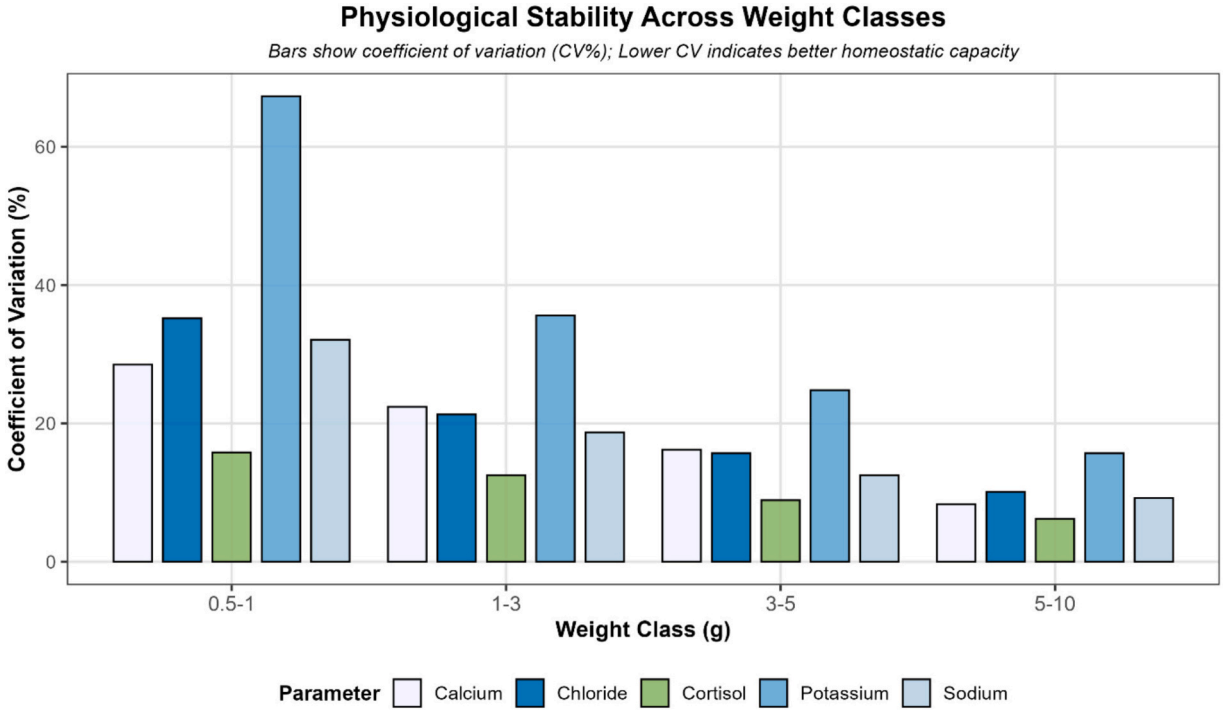

Fig. 13. Physiological stability across weight classes expressed as coefficient of variation (CV%). Bars represent the coefficient of variation (CV = SD/mean × 100) for each physiological parameter calculated across the four salinities (0, 4, 8, 12 ppt). Lower CV values indicate better homeostatic capacity, meaning the parameter remains stable regardless of environmental salinity.

2006; Emeish et al., 2023). These findings indicate that histological injury was not strictly monotonic with body size and should be interpreted together with the physiological data. The branchial lesions observed here also match previous sturgeon studies showing salinity-induced gill remodelling, including chloride-cell proliferation and structural changes associated with osmotic acclimation. Taken together, the histological evidence supports the interpretation that smaller juveniles are less able to preserve tissue integrity during salinity challenge (Rodriguez et al., 2002; He et al., 2009; Shirangi et al., 2016). The renal lesions were equally important, as they indicate that salinity challenge impacted both filtration and tubular function. The kidney's role in water and ion balance makes it critical for osmoregulatory shifts; under increased salinity, kidneys must reduce urine volume and excrete excess ions, which can stress nephron epithelia (Takvam et al., 2021). We observed glomerular expansion, tubular obstruction and necrosis, hypertrophy, congestion, hemorrhage and hemosiderin deposition, all signs of impaired renal function and cellular injury. Some lesions were already present in freshwater controls, especially in the smallest and largest juveniles, suggesting baseline developmental stress or ontogenetic sensitivity (Singh, 2018; Ali et al., 2024). With higher salinity, renal damage intensified, reflecting osmotic overload on nephron structures. Comparable renal degeneration has been described in carp, tilapia, and other fishes under ionic stress (Ding et al., 2023; Ali et al., 2024). The lymphoid proliferation and hemosiderin likely reflect

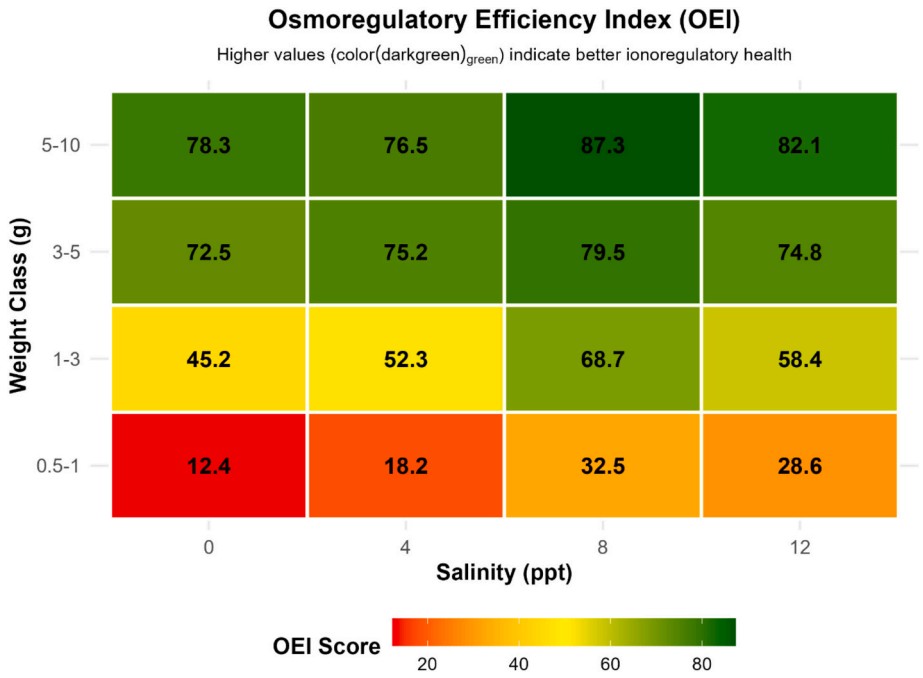

Fig. 14. Osmoregulatory Efficiency Index (OEI) in stellate sturgeon juveniles. The OEI is a composite measure of ionoregulatory health calculated as: OEI = 100 - (Na_deviation + K_deviation + Cl_deviation)/3, where deviation = |measured - ideal|/ideal × 100. Higher OEI values (green) indicate better ionoregulatory capacity. (For interpretation of the references to colour in this figure legend, the reader is referred to the web version of this article.)

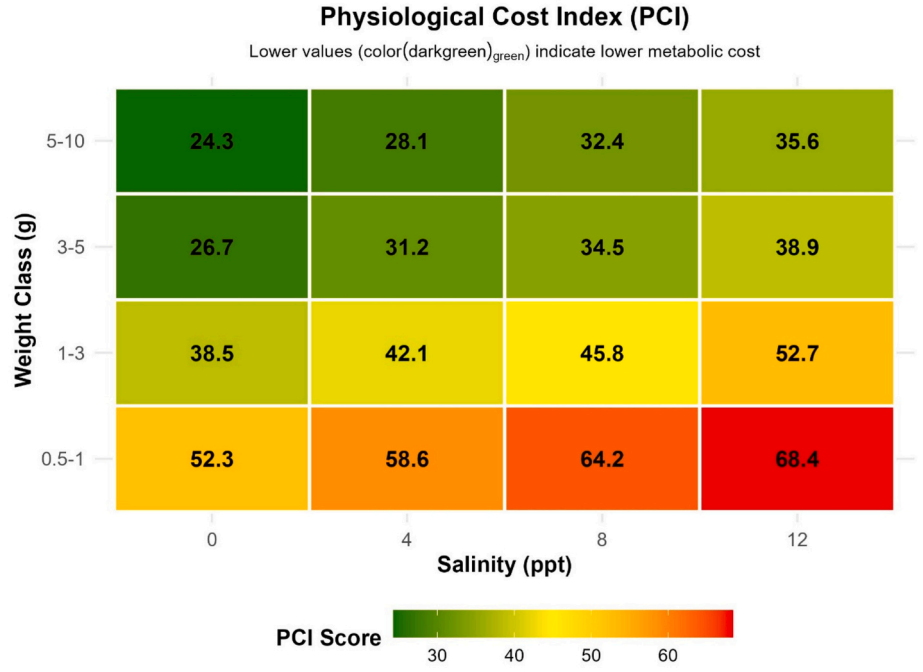

Fig. 15. Physiological Cost Index (PCI) in stellate sturgeon juveniles. The PCI quantifies the metabolic cost of osmoregulation, integrating stress response (cortisol) and ion regulatory deviation. Colour Scale: Green (PCI < 30): Minimal cost - optimal energy efficiency; Yellow (PCI 30–50): Moderate cost - acceptable energy expenditure; Red (PCI > 50): High cost - significant energy expenditure. (For interpretation of the references to colour in this figure legend, the reader is referred to the web version of this article.)

chronic injury and immune activation (Lee et al., 2009; Hossain et al., 2022; Zhou et al., 2023). Overall, the kidney findings corroborate the blood biochemistry: juveniles with poorer Na^+ and K^+ regulation and higher cortisol also showed more extensive organ damage, indicating compromised filtration and ion transport capacity. Histopathological severity should be interpreted alongside the physiological data, because some larger juveniles showed substantial baseline lesions in control conditions; therefore, tissue injury was not strictly monotonic with body size, and it should not be used alone as a proxy for salinity tolerance. Taken together, the histological results support an empirical transition zone around 3 g under the tested conditions rather than a strict physiological breakpoint.

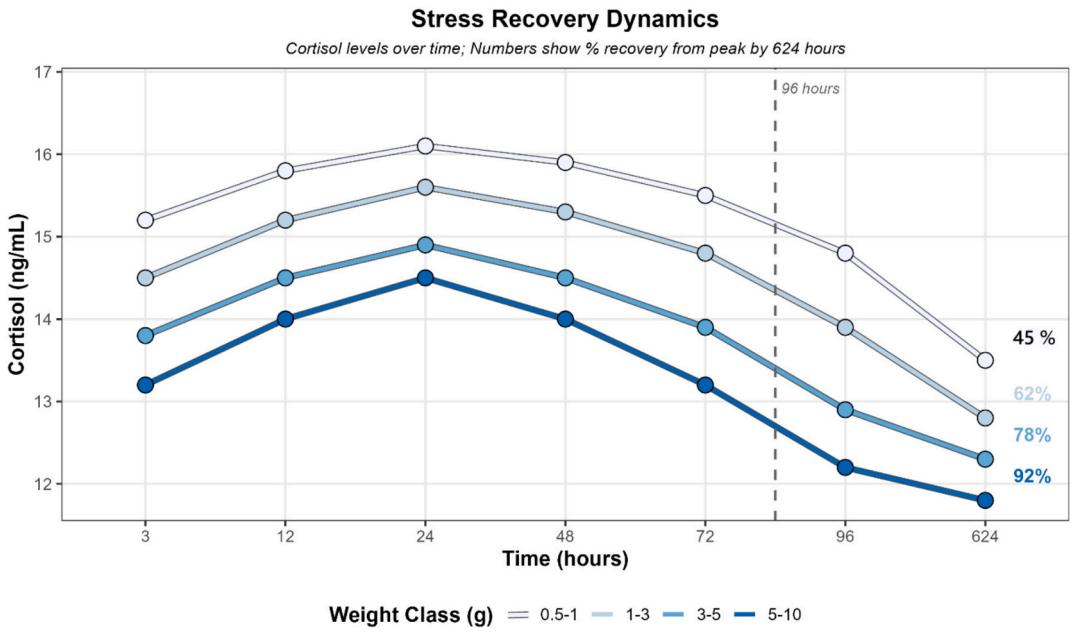

Fig. 16. Stress recovery dynamics in stellate sturgeon juveniles across four weight classes. Lines show mean cortisol levels (ng/mL) over 624 h following exposure to salinity challenges. Data represents the average across all salinities (0, 4, 8, 12 ppt), as the temporal pattern was consistent across treatments. The vertical dashed line at 96 h indicates the point where larger fish had already achieved significant recovery. Numbers at the end of each line indicate the percentage recovery from peak stress achieved by 624 h.

The size-dependent survival pattern provides the most direct management implication. Mortality declined sharply with increasing body size, with fish >3 g surviving far better than those <3 g at all salinities. Under the present experimental conditions, fish >3 g showed lower mortality than fish <3 g. This pattern is consistent with previous sturgeon studies showing that salinity tolerance and survival increase with body size and developmental stage. For example, juvenile Russian sturgeon and Persian sturgeon exhibited higher survival and better osmotic regulation as body size increased, and in one Persian sturgeon study fish under 3 g could not survive increased salinity, whereas larger juveniles acclimated more successfully. Similar age- and size-dependent improvements in osmoregulatory performance were also reported for juvenile green sturgeon, where hyperosmotic adaptability increased with growth (Krayushkina and Semenova, 2006; Allen and Cech Jr, 2007; Farabi et al., 2011; Shirangi et al., 2016). From a conservation perspective, the key question is not just whether a given salinity is tolerable, but whether juveniles of a given size can survive it with acceptable physiological cost. Exploratory composite indices were broadly consistent with this interpretation, with the highest scores generally occurring in larger juveniles, especially under freshwater or low-brackish conditions associated with lower physiological disturbance. Because the study compared discrete weight classes rather than a continuous size gradient, the approximate 3 g value should be interpreted as an empirical transition zone and a practical management benchmark under the conditions tested, rather than as a definitive physiological breakpoint. The composite indices (OEI, PCI, SRI, and OHI) were broadly concordant with the univariate results; however, because these indices were author-defined and not externally validated, they are interpreted here only as exploratory summary tools (Allen and Cech Jr, 2007; Farabi et al., 2011; Shirangi et al., 2016). Collectively, these comparisons support interpreting ~3 g as an empirical transition zone rather than a fixed physiological breakpoint, as similar size-dependent improvements in salinity tolerance have been reported across multiple sturgeon species (Allen and Cech Jr, 2007; Farabi et al., 2011; Shirangi et al., 2016).

Taken together, the results support three main conclusions. First, plasma Na^+ (and by extension Cl^-) and cortisol are the most informative systemic markers of salinity challenge in juvenile *A. stellatus*. Second, gill and kidney histology reveal that salinity stress incurs significant tissue injury, especially in smaller juveniles, and some larger fish may exhibit pre-existing pathology. Third, a body-size threshold near ~3 g separates juveniles with limited tolerance from those with substantially better osmoregulatory capacity. The mixed live prey used in this study were consistent with standard sturgeon hatchery practice and were provided uniformly across treatments to minimize dietary bias. Live food is recommended during early sturgeon rearing to support feeding initiation and gradual acclimation to captive conditions (Chebanov et al., 2011). The prey mixture used here comprised nutritionally rich natural items: *Gammarus pulex* meal has been reported to contain about 40% crude protein and 5.5% crude fat (dry matter basis), *Chironomus albidus* larvae about 55.7% crude protein and 9.7% lipid (dry matter basis), and *H. diversicolor* about 54–58% protein and 12–16% lipid (dry matter basis) (Ashour et al., 2021; Pajand et al., 2026). Because prey was not chemically analyzed in the present study, exact mineral intake cannot be quantified retrospectively; however, the diet was standardized across all experimental groups, so any prey-related nutritional variation would not explain the between-treatment differences observed. These findings have direct relevance to hatchery and release strategies: releasing fish below the approximate 3 g transition zone into brackish water is likely to result in higher mortality and should be avoided. Conversely, using larger juveniles and allowing for gradual acclimation to salinity changes (for example, by staging releases) could enhance survival and support restoration efforts. Importantly, this interpretation is based on discrete size classes and therefore should be viewed as a management-oriented approximation rather than a fixed physiological cutoff. Practical management recommendations can therefore be proposed. For release into estuarine or brackish environments, juveniles should preferably be stocked at >3 g body weight, as fish below this threshold showed poorer physiological performance and higher mortality. Where transfer to saline water is required, hatcheries should apply a stepwise salinity acclimation protocol rather than direct transfer, with gradual increases over several days before release. Nursery systems should prioritize rapid but healthy growth to the target release size through appropriate stocking densities, stable dissolved

oxygen, temperature control, regular water exchange, and adequate feeding. In addition, release timing and locations should consider local salinity conditions, with preference for periods or sites of lower salinity to reduce osmotic challenge during the immediate post-release phase.

5. Conclusion

This study demonstrates that salinity tolerance in juvenile stellate sturgeon is strongly size dependent. Fish around or above 3 g showed substantially better osmoregulatory stability, lower cortisol responses, reduced histopathological damage, and lower mortality under salinity challenge compared with smaller juveniles. Na^+ was the principal ion associated with osmotic disturbance, whereas K^+ reflected greater physiological instability in smaller fish. Semi-quantitative histopathological analysis confirmed significant salinity- and size-dependent damage in both gill and kidney tissues. Overall, the results identify an empirical transition zone near 3 g under the tested conditions, above which juveniles exhibit greater physiological resilience to brackish-water exposure. These findings support the use of gradual salinity acclimation and preferential release of larger juveniles to improve stocking success and conservation outcomes.

CRediT authorship contribution statement

Zabih Ollah Pajand: Writing – review & editing, Validation, Project administration, Methodology, Investigation, Formal analysis, Data curation, Conceptualization. **Esmaeil Hosseinnia:** Methodology, Investigation, Formal analysis. **Naghmeh Jafari Pastaki:** Writing – review & editing, Writing – original draft, Visualization, Validation. **Ali Hallajian:** Formal analysis. **Ayoub Yousefi:** Methodology, Investigation. **Arash Lebria:** Methodology, Formal analysis. **Alireza Ashori:** Methodology, Investigation, Formal analysis. **Hamed Abdollahpour:** Writing – review & editing, Writing – original draft, Visualization, Validation, Software, Data curation, Conceptualization.

Funding

This research was supported by the Iranian Fisheries Research Organization (IFRO) under project number (12-32-12-008-98004-980153).

Declaration of competing interest

The authors declare no conflicts of interest.

Acknowledgement

The authors gratefully acknowledge the International Sturgeon Research Institute, Iranian Fisheries Science Research Institute, and the Agricultural Research Education and Extension Organization (AREEO), Rasht, Guilan, Iran, for financial and technical support. We thank the staff of the Guilan Sturgeon Research Station (Chaboksar, Iran) for assistance with fish husbandry and sampling, and the veterinary team at the Shahid Beheshti Stock Restoration and Propagation Centre for providing certified fish stocks.

Data availability

The datasets used and/or analyzed during the current study are available from the corresponding author on reasonable request.

References

Abdollahpour, H., Pastaki, N.J., Falahatkar, B., 2025. The interplay between thyroxine and cortisol in zebrafish: effects on growth, physiology, and reproduction. Anim. Reprod. Sci. 274, 107795. https://doi.org/10.1016/j.anireprosci.2025.107795.

Abdollahpour, H., Karimzadeh, M., Pastaki, N.J., Zamani, H., 2026. The antithyroid drug methimazole as an emerging aquatic contaminant: physiological and reproductive disruption in female goldfish (*Carassius auratus*) and partial mitigation by thyroxine. Emerg. Contam., 100626 https://doi.org/10.1016/j.emcon.2026.100626.

Ali, A., Azom, M.G., Sarker, B.S., Rani, H., Alam, M.S., Islam, M.S., 2024. Repercussion of salinity on hematological parameters and tissue morphology of gill and kidney at early life of tilapia. Aquac. Fish. 9 (2), 256–264. https://doi.org/10.1016/j.aaf.2022.04.006.

Allen, P.J., Cech Jr., J.J., 2007. Age/size effects on juvenile green sturgeon, *Acipenser medirostris*, oxygen consumption, growth, and osmoregulation in saline environments. Environ. Biol. Fish 79 (3), 211–229. https://doi.org/10.1007/s10641-006-9049-9.

Allen, P.J., Cech Jr., J.J., Kültz, D., 2009. Mechanisms of seawater acclimation in a primitive, anadromous fish, the green sturgeon. J. Comp. Physiol. B. 179 (7), 903–920. https://doi.org/10.1007/s00360-009-0372-2.

Allen, P.J., McEnroe, M., Forostyan, T., Cole, S., Nicholl, M.M., Hodge, B., Cech Jr., J.J., 2011. Ontogeny of salinity tolerance and evidence for seawater-entry preparation in juvenile green sturgeon, *Acipenser medirostris*. J. Comp. Physiol. B. 181 (8), 1045–1062. https://doi.org/10.1007/s00360-011-0592-0.

Alsafy, M.A., Abd-Elhafeez, H.H., Rashwan, A.M., Erasha, A., Ali, S., El-Gendy, S.A., 2025. Anatomy, histology, and morphology of fish gills in relation to feeding habits: a comparative review of marine and freshwater species. BMC Zool. 10 (1), 3. https://doi.org/10.1186/s40850-025-00223-5.

Amiri, B.M., Baker, D.W., Morgan, J.D., Brauner, C.J., 2009. Size dependent early salinity tolerance in two sizes of juvenile white sturgeon, *Acipenser transmontanus*. Aquaculture 286 (1–2), 121–126. https://doi.org/10.1016/j.aquaculture.2008.08.037.

Ashour, M., Abo-Taleb, H.A., Hassan, A.K.M., Abdelzaher, O.F., Mabrouk, M.M., Elokaby, M.A., Mansour, A.T., 2021. Valorization use of amphipod meal, Gammarus pulex, as a fishmeal substitute on growth performance, feed utilization, histological and histometric indices of the gut, and economic revenue of grey mullet. J. Mar. Sci. Eng. 9 (12), 1336. https://doi.org/10.3390/jmse9121336.

Barany, A., Shaughnessy, C.A., Fuentes, J., Mancera, J.M., McCormick, S.D., 2020. Osmoregulatory role of the intestine in the sea lamprey (*Petromyzon marinus*). Am. J. Phys. Regul. Integr. Comp. Phys. 318 (2), R410–R417. https://doi.org/10.1152/ajpregu.00033.2019.

Barton, B.A., 2002. Stress in fishes: a diversity of responses with particular reference to changes in circulating corticosteroids. Integr. Comp. Biol. 42 (3), 517–525. https://doi.org/10.1093/icb/42.3.517.

Billard, R., Lecointre, G., 2000. Biology and conservation of sturgeon and paddlefish. Rev. Fish Biol. Fish. 10 (4), 355–392. https://doi.org/10.1023/A:1012231526151.

Chebanov, M., Rosenthal, H., Gessner, J., Van Anrooy, R., Doukakis, P., Pourkazemi, M., Williot, P., 2011. Sturgeon Hatchery Practices and Management for Release-Guidelines FAO Fisheries and Aquaculture Technical Paper No 570. FAO, Ankara, 2011; 110p, ISBN 978-92-5-107044-4. Available online. https://www.fao.org/4/i2428e/i2428e.pdf. accessed on 8 August 2024.

Dawood, M.A., Noreldin, A.E., Sewilam, H., 2022. Blood biochemical variables, antioxidative status, and histological features of intestinal, gill, and liver tissues of African catfish (*Clarias gariepinus*) exposed to high salinity and high-temperature stress. Environ. Sci. Pollut. Res. 29 (37), 56357–56369. https://doi.org/10.1007/s11356-022-19702-0.

Ding, L., Liu, Y., Wei, X., Geng, C., Liu, W., Han, L., Sun, Y., 2023. Effects of saline-alkaline stress on metabolome, biochemical parameters, and histopathology in the kidney of crucian carp (*Carassius auratus*). Metabolites 13 (2), 159. https://doi.org/10.3390/metabo13020159.

Downie, A.T., Wallace, H., Taylor, S., Kieffer, J.D., 2018. The impact of acute salinity exposure and temperature on the survival, osmoregulation, and hematology of juvenile shortnose sturgeon (*Acipenser brevirostrum*). Can. J. Zool. 96 (8), 913–919. https://doi.org/10.1139/cjz-2017-0149.

Emeish, W.F., Abd-ElHafeez, H.H., Alghamdi, A.A., Ahmed, M., Khalifa, M.O., El-Mansi, A.A., Soliman, S.A., 2023. Morphological changes in intraepithelial and stromal telocytes in *Cyprinus carpio* in response to salinity stress. Sci. Rep. 13 (1), 19987. https://doi.org/10.1038/s41598-023-43279-4.

Evans, D.H., Claiborne, J.B., 2009. Osmotic and ionic regulation in fishes. In: Evans, D.H. (Ed.), Osmotic and Ionic Regulation: Cells and Animals. CRC Press, Boca Raton, FL, pp. 295–366.

Evans, D.H., Piermarini, P.M., Choe, K.P., 2005. The multifunctional fish gill: dominant site of gas exchange, osmoregulation, acid-base regulation, and excretion of nitrogenous waste. Physiol. Rev. 85 (1), 97–177. https://doi.org/10.1152/physrev.00050.2003.

Falahatkar, B., Abdollahpour, H., Jafari, N., 2022. Physiological responses to air exposure stress in Siberian sturgeon (*Acipenser baerii* Brandt 1869) injected with dexamethasone. J. Appl. Ichthyol. 38 (3), 311–319. https://doi.org/10.1111/jai.14321.

Farabi, S.M.V., Najafpour, S., Ghiasi, M., Samadi, H., 2011. Initial salinity tolerance and ion-osmotic parameters in juvenile Russian sturgeon, *Acipenser gueldenstaedtii*, Brandt, 1833. Iran. J. Fish. Sci. 10 (4), 607–615.

Fiol, D.F., Chan, S.Y., Kültz, D., 2006. Regulation of osmotic stress transcription factor 1 (Ostf1) in tilapia (*Oreochromis mossambicus*) gill epithelium during salinity stress. J. Exp. Biol. 209 (16), 3257–3265. https://doi.org/10.1242/jeb.02352.

Florescu, I.E., Georgescu, S.E., Dudu, A., Balaş, M., Voicu, S., Grecu, I., Costache, M., 2021. Oxidative stress and antioxidant defense mechanisms in response to starvation and refeeding in the intestine of stellate sturgeon (*Acipenser stellatus*) juveniles from aquaculture. Animals 11 (1), 76. https://doi.org/10.3390/ani11010076.

Gonzalez, R.J., 2012. The physiology of hyper-salinity tolerance in teleost fish: a review. J. Comp. Physiol. B. 182 (3), 321–329. https://doi.org/10.1007/s00360-011-0624-9.

Guo, B., Tang, Z., Wu, C., Xu, K., Qi, P., 2018. Transcriptomic analysis reveal an efficient osmoregulatory system in Siberian sturgeon *Acipenser baeri* in response to salinity stress. Sci. Rep. 8 (1), 14353. https://doi.org/10.1038/s41598-018-32771-x.

He, X., Zhuang, P., Zhang, L., Xie, C., 2009. Osmoregulation in juvenile Chinese sturgeon (*Acipenser sinensis* gray) during brackish water adaptation. Fish Physiol. Biochem. 35 (2), 223–230. https://doi.org/10.1007/s10695-008-9230-5.

Hossain, F., Islam, S.M., Islam, M.S., Shahjahan, M., 2022. Behavioral and histo-pathological indices of striped catfish (*Pangasionodon hypophthalmus*) exposed to different salinities. Aquacult. Rep. 23, 101038. https://doi.org/10.1016/j.aqrep.2022.101038.

Jafari, N., Abdollahpour, H., Falahatkar, B., 2020. Stimulatory effects of short-term calcitonin administration on plasma calcium, magnesium, phosphate, and glucose in juvenile Siberian sturgeon *Acipenser baerii*. Fish Physiol. Biochem. 46 (4), 1443–1449. https://doi.org/10.1007/s10695-020-00801-z.

Jamshidi, S., Abu Bakar, N.B., 2012. Seasonal variations in temperature, salinity and density in the southern coastal waters of the Caspian Sea. Oceanology 52 (3), 380–396. https://doi.org/10.1134/S0001437012030034.

Jarić, I., Riepe, C., Gessner, J., 2018. Sturgeon and paddlefish life history and management: experts' knowledge and beliefs. J. Appl. Ichthyol. 34 (2), 244–257. https://doi.org/10.1111/jai.13563.

Kammerer, B.D., Cech Jr., J.J., Kültz, D., 2010. Rapid changes in plasma cortisol, osmolality, and respiration in response to salinity stress in tilapia (*Oreochromis mossambicus*). Comp. Biochem. Physiol. A Mol. Integr. Physiol. 157 (3), 260–265. https://doi.org/10.1016/j.cbpa.2010.07.009.

Kazemi, R., Bahmani, M., Krayushkina, L.S., Pourkazemi, M., Ogorzalek, A., 2003. Changes in blood serum osmolarity and ultrastructure of gill chloride cells in young Persian sturgeon *Acipenser persicus* (Borodin) of different sizes during adaptation to sea water. Zool. Pol. 48 (1–4), 5–30.

Krayushkina, L.S., Semenova, O.G., 2006. Osmotic and ion regulation in different species of acipenserids (Acipenseriformes, Acipenseridae). J. Ichthyol. 46 (1), 108–119. https://doi.org/10.1134/S0032945206010139.

Krayushkina, L.S., Panov, A.A., Gerasimov, A.A., Potts, W.T.W., 1996. Changes in sodium, calcium and magnesium ion concentrations in sturgeon (*Huso huso*) urine and in kidney morphology. J. Comp. Physiol. B. 165 (7), 527–533. https://doi.org/10.1007/BF00387513.

Krayushkina, L.S., Semenova, O.G., Vyushina, A.V., Gerasimov, A.A., 2015. Morphofunctional remodelling of the osmoregulatory system in starred sturgeon *Acipenser stellatus* (Acipenseridae) during transition from hyperosmotic to hypoosmotic regulation. J. Ichthyol. 55 (2), 259–272. https://doi.org/10.1134/S0032945215020101.

Kültz, D., 2015. Physiological mechanisms used by fish to cope with salinity stress. J. Exp. Biol. 218 (12), 1907–1914. https://doi.org/10.1242/jeb.118695.

LeBreton, G.T., Beamish, F.W.H., 1998. The influence of salinity on ionic concentrations and osmolarity of blood serum in lake sturgeon, *Acipenser fulvescens*. Environ. Biol. Fish 52 (4), 477–482. https://doi.org/10.1023/A:1007421410090.

Lee, K.S., Groshong, S.D., Cool, C.D., Kleinschmidt-DeMasters, B.K., van Dyk, L.F., 2009. Murine gammaherpesvirus 68 infection of IFNγ unresponsive mice: a small animal model for gammaherpesvirus-associated B-cell lymphoproliferative disease. Cancer Res. 69 (13), 5481–5489. https://doi.org/10.1158/0008-5472.CAN-09-0291.

Lee, C.E., Charmantier, G., Lorin-Nebel, C., 2022. Mechanisms of Na+ uptake from freshwater habitats in animals. Front. Physiol. 13, 1006113. https://doi.org/10.3389/fphys.2022.1006113.

McCormick, S.D., 2001. Endocrine control of osmoregulation in teleost fish. Am. Zool. 41 (4), 781–794. https://doi.org/10.1093/icb/41.4.781.

McCormick, S.D., 2011. The hormonal control of osmoregulation in teleost fish. In: Farrell, A.P. (Ed.), Encyclopedia of Fish Physiology: From Genome to Environment. Academic Press, San Diego, pp. 1466–1473. https://doi.org/10.1016/B978-0-12-374553-8.00212-4.

McCormick, S.D., Taylor, M.L., Regish, A.M., 2020. Cortisol is an osmoregulatory and glucose-regulating hormone in Atlantic sturgeon, a basal ray-finned fish. J. Exp. Biol. 223 (18), jeb220251. https://doi.org/10.1242/jeb.220251.

McEnroe, M., Cech Jr., J.J., 1985. Osmoregulation in juvenile and adult white sturgeon, *Acipenser transmontanus*. Environ. Biol. Fish 14 (1), 23–30. https://doi.org/10.1007/BF00001573.

McLean, M.F., Hanson, K.C., Cooke, S.J., Hinch, S.G., Patterson, D.A., Nettles, T.L., Crossin, G.T., 2016. Physiological stress response, reflex impairment and delayed mortality of white sturgeon Acipenser transmontanus exposed to simulated fisheries stressors. Conserv. Physiol. 4 (1), cow031. https://doi.org/10.1093/conphys/cow031.

Pajand, Z.O., Haddadi Moghaddam, K., Chubian, F., Farzaneh, E., Hosseinnia, E., 2022. Effects of dietary various oil sources on zootechnical performance, sexual maturation, whole-body proximate composition and fatty acid profile of *Hediste diversicolor*. Aquac. Res. 53 (8), 3078–3089. https://doi.org/10.1111/are.15820.

Pajand, Z., Yousefi, A., Abdollahpour, H., Hosseinnia, E., Lebria, A., Golalipour, Y., Pastaki, N.J., Pourgholam, M., 2026. Diet and density effects on growth, proximate composition and fatty-acid profile of *Hediste diversicolor* juveniles. PLoS One 21 (4), e0344444. https://doi.org/10.1371/journal.pone.0344444.

Pastaki, N.J., Abdollahpour, H., Falahatkar, B., 2025. Developmental responses of sterlet (*Acipenser ruthenus*) to temperature modulation with insights into intestinal and morphological traits. Sci. Rep. 15 (1), 18170. https://doi.org/10.1038/s41598-025-02566-y.

Rodriguez, A., Gallardo, M.A., Gisbert, E., Santilari, S., Ibarz, A., Sanchez, J., Castello-Orvay, F., 2002. Osmoregulation in juvenile Siberian sturgeon (*Acipenser baerii*). Fish Physiol. Biochem. 26 (4), 345–354. https://doi.org/10.1023/B:FISH.0000009263.83075.68.

Sarpanah, A., Pajand, Z., Yousefi, S., Hassani, M.H.S., Jourdehi, A.Y., Vaghei, R.G., Sohrabi, T., 2026. Impact of different weaning strategies on growth indices, biochemical composition, and digestive enzyme activity in stellate sturgeon (*Acipenser stellatus*) larvae. Anim. Feed Sci. Technol. 312, 116696. https://doi.org/10.1016/j.anifeedsci.2026.116696.

Shartau, R.B., Shu, J., Baker, D.W., 2023. The role of salinity in recovery of white sturgeon (*Acipenser transmontanus*) from stimulated angling stress. Conserv. Physiol. 11 (1), coad009. https://doi.org/10.1093/conphys/coad009.

Shirangi, S.A., Kalbassi, M.R., Khodabandeh, S., Jafarian, H., Lorin-Nebel, C., Farcy, E., Lignot, J.H., 2016. Salinity effects on osmoregulation and gill morphology in juvenile Persian sturgeon (*Acipenser persicus*). Fish Physiol. Biochem. 42 (6), 1741–1754. https://doi.org/10.1007/s10695-016-0254-y.

Singh, G., 2018. Salinity Tolerance and Stress Responses of Freshwater Carp, *Cyprinus carpio* Linn. (Common carp) in Inland Saline Water. Doctoral dissertation. Guru Angad Dev Veterinary and Animal Sciences University.

Taghizadeh Rahmat Abadi, Z., Khodabandeh, S., Abtahi, B., Charmantier, G., Charmantier-Daures, M., 2011. Ultrastructure and osmoregulatory function of the kidney in larvae of the Persian sturgeon *Acipenser persicus*. J. Fish Biol. 78 (5), 1359–1374. https://doi.org/10.1111/j.1095-8649.2011.02939.x.

Takvam, M., Wood, C.M., Kryvi, H., Nilsen, T.O., 2021. Ion transporters and osmoregulation in the kidney of teleost fishes as a function of salinity. Front. Physiol. 12, 664588. https://doi.org/10.3389/fphys.2021.664588.

Thibaut, L.H., Emilie, F., Béatrice, C., Romain, G., François, R., Sophie, H., Catherine, L. N., 2019. Are European sea bass as euryhaline as expected? Intraspecific variation in freshwater tolerance. Mar. Biol. 166 (8), 102. https://doi.org/10.1007/s00227-019-3551-z.

Vahdatiraad, L., Heidari, B., Zarei, S., Sohrabi, T., Ghafouri, H., 2023. Biological responses of stellate sturgeon fingerlings (*Acipenser stellatus*) immersed in HSP inducer to salinity changes. Mar. Environ. Res. 191, 106145. https://doi.org/10.1016/j.marenvres.2023.106145.

Wang, J., Zhu, X., Sun, Y., Gu, L., Wu, Y., Chen, Y., Yang, Z., 2022. Changes in transcriptome and ultrastructure reveal salinity tolerance of obscure puffer *Takifugu obscurus*. Front. Mar. Sci. 9, 854140. https://doi.org/10.3389/fmars.2022.854140.

Wassink, L., Huerta, B., Larson, D., Li, W., Scribner, K., 2022. Hatchery and wild larval lake sturgeon experience effects of captivity on stress reactivity, behavior and predation risk. Conserv. Physiol. 10 (1), coac062. https://doi.org/10.1093/conphys/coac062.

Wendelaar Bonga, S.E., 1997. The stress response in fish. Physiol. Rev. 77 (3), 591–625. https://doi.org/10.1152/physrev.1997.77.3.591.

Xenarios, S., Orazgaliyev, S., Torabi Haghighi, A., Kløve, B., 2025. A perspective on sustainability and environmental challenges in the Caspian Sea. Int. J. Water Resour. Dev. 41 (1), 1–8. https://doi.org/10.1080/07900627.2025.2441052.

Yuan, Z., Li, Y., Li, Y., Gao, P., Jia, C., Meng, Q., Lai, Q., 2026. Effects of low salinity stress on the survival and osmotic regulation of two sizes of juvenile *Acanthopagrus schlegelii*. Mar. Biotechnol. 28 (2), 40. https://doi.org/10.1007/s10126-026-10589-3.

Zhou, Q., Cui, J., Liu, Y., Gu, L., Teng, X., Tang, Y., 2023. EGCG alleviated Mn exposure-caused carp kidney damage via trpm2-NLRP3-TNF-α-JNK pathway: oxidative stress, inflammation, and tight junction dysfunction. Fish Shell Immunol. 134, 108582. https://doi.org/10.1016/j.fsi.2023.108582.